Bioorganic Chemistry 115 (2021) 105236

Contents lists available at ScienceDirect

Bioorganic Chemistry

journal homepage: www.elsevier.com/locate/bioorg

Novel tetrahydrobenzo[*b*]thiophen-2-yl)urea derivatives as novel α-glucosidase inhibitors: Synthesis, kinetics study, molecular docking, and *in vivo* anti-hyperglycemic evaluation

Hong-Xu Xie [a,1], Juan Zhang [a,1], Yue Li [a], Jin-He Zhang [a], Shan-Kui Liu [a], Jie Zhang [b], Hua Zheng [b], Gui-Zhou Hao [b,*], Kong-Kai Zhu [a,c,*], Cheng-Shi Jiang [a,*]

[a] School of Biological Science and Technology, University of Jinan, Jinan 250022, China
[b] Lunan Pharmaceutical Group Co., Ltd., Linyi 273400, China
[c] Drug Discovery and Design Center, State Key Laboratory of Drug Research, Shanghai Institute of Materia Medica, Chinese Academy of Sciences, Shanghai, China

ARTICLE INFO

Keywords:
Tetrahydrobenzo[*b*]thiophen-2-yl)urea
α-Glucosidase inhibitors
Non-competitive inhibitor
Molecular docking
Anti-hyperglycaemic activity
Type 2 diabetes

ABSTRACT

α-Glucosidase inhibitors, which can inhibit the digestion of carbohydrates into glucose, are one of important groups of anti-type 2 diabetic drugs. In the present study, we report our effort on the discovery and optimization of α-glucosidase inhibitors with tetrahydrobenzo[*b*]thiophen-2-yl)urea core. Screening of an in-house library revealed a moderated α-glucosidase inhibitors, **5a**, and then the following structural optimization was performed to obtain more efficient derivatives. Most of these derivatives showed increased inhibitory activity against α-glucosidase than the parental compound **5a** (IC_{50} of 26.71 ± 1.80 μM) and the positive control acarbose (IC_{50} of 258.53 ± 1.27 μM). Among them, compounds **8r** (IC_{50} = 0.59 ± 0.02 μM) and **8s** (IC_{50} = 0.65 ± 0.03 μM) were the most potent inhibitors, and showed selectivity over α-amylase. The direct binding of both compounds with α-glucosidase was confirmed by fluorescence quenching experiments. Kinetics study revealed that these compounds were non-competitive inhibitors, which was consistent with the molecular docking results that compounds **8r** and **8s** showed high preference to bind to the allosteric site instead of the active site of α-glucosidase. In addition, compounds **8r** and **8s** were not toxic (IC_{50} > 100 μM) towards LO2 and HepG2 cells. Finally, the *in vivo* anti-hyperglycaemic activity assay results indicated that compounds **8r** could significantly decrease the level of plasma glucose and improve glucose tolerance in SD rats treated with sucrose. The present study provided the tetrahydrobenzo[*b*]thiophen-2-yl)urea chemotype for developing novel α-glucosidase inhibitors against type 2 diabetes.

1. Introduction

Type 2 diabetes mellitus (T2DM) is a chronic metabolic disorder characterized by insulin resistance and pancreatic islet β-cell failure [1], and accounts for 80% to 90% of all diabetic patients [2]. According to the statistics of the International Diabetes Federation report, about 403 million people were diagnosed with diabetes in 2019 worldwide, and its prevalence was estimated to be 700 million by 2045 [3]. Diabetes can increase the risk of various health complications, including stroke [4,5], peripheral artery disease [6], and cancer [7], and it also affects the kidneys, heart, and nerves by causing varying degrees of damage [8].

The main strategy for controlling diabetes is to lower the level of blood glucose [9]. The glucose in the blood comes from the hydrolysis of carbohydrates catalyzed by enzymes such as α-glucosidase and α-amylase [10]. α-Glucosidase is a key glycoside hydrolase specifically hydrolyzing 1,4-α-glucopyranosides bond to produce α-glucose [11,12]. Inhibition of α-glucosidase could retard the absorption of carbohydrates at the small intestine and reduce the postprandial blood glucose levels [13,14], while side effects including flatulence are possible as a consequence of bacterial fermentation if simultaneous strong inhibition of α-amylases by drugs result in undigested polysaccharides entering the colon [15,16]. Moreover, α-glucosidase inhibitors have been marketed as therapeutic drugs for T2DM. Thus, α-glucosidase enzyme was taken as one of the most promising targets for the treatment of diabetes [17].

* Corresponding authors at: School of Biological Science and Technology, University of Jinan, Jinan 250022, China (C.-S. Jiang).
E-mail addresses: haoguizhouhgz@163.com (G.-Z. Hao), bio_zhukk@ujn.edu.cn (K.-K. Zhu), bio_jiangcs@ujn.edu.cn (C.-S. Jiang).
[1] These authors contributed equally to this work.

https://doi.org/10.1016/j.bioorg.2021.105236
Received 27 May 2021; Received in revised form 26 July 2021; Accepted 1 August 2021
Available online 8 August 2021

Attracted by the important biological properties of α-glucosidase, medicinal chemists have developed a variety of α-glucosidase inhibitors [17–30]. Currently, three approved α-glucosidase inhibitors are carbohydrate mimics, including acarbose, voglibose, and miglitol (Fig. 1) used in reducing postprandial hyperglycemia [17,31–33]. However, some undesired effects, including flatulence, diarrhea, and stomach ache, limited their clinical application [34]. Therefore, there is an urgent need to discover novel α-glucosidase inhibitors to overcome these side effects.

In our project to identify new α-glucosidase inhibitors [35,36], our in-house compounds were screened for their activities towards α-glucosidase at an initial concentration of 100 μM, with acarbose as a positive control. The preliminary results of bioassay revealed that a compound **5a** possessing tetrahydrobenzo[*b*]thiophen-2-yl)urea core showed 87.76% inhibitory activity against α-glucosidase, and its IC_{50} value was determined to be 26.71 ± 1.80 μM. To further improve the α-glucosidase inhibitory activity of **5a**, a systematic structural modification was carried out. In this study, a series of thiophen- and thiazole-urea derivatives were synthesized and evaluated for their activities, and the structure–activity relationships (SAR) study was discussed. Further, the direct binding of the most potent compounds **8r** and **8s** with α-glucosidase was confirmed by fluorescence quenching experiments, and their inhibition mechanisms were investigated using molecular docking and kinetic studies. Finally, the *in vitro* cytotoxicity and *in vivo* anti-hyperglycemic effect of **8r** and **8s** were also evaluated. Herein, we report the synthesis, *in vitro* and *in vivo* biological evaluations of a series of tetrahydrobenzo[*b*]thiophen-2-yl)urea-based novel α-glucosidase inhibitors.

2. Results and discussion

2.1. Chemical synthesis

The synthetic routes of the target thiophen- and thiazole-urea derivatives are outlined in Schemes 1–3, and their structures are displayed in Tables 1–3. As shown in Scheme 1, the synthetic intermediates **2a-2k** were obtained by the reaction of compounds **1a-1d** with cyanoacetate or the reaction of **1a-1g** with malononitrile in the presence of sulfur [37]. *p*-Methoxybenzyl amine **3a** is reacted with *N,N'*-carbonyldiimidazole (CDI) to form intermediate **4a** [38], which was then reacted with **2a-2k** to afford the thiophen-urea derivatives **5a-5k**, while the thiazole-urea derivatives **5l-5n** were obtained by treating **4a** with the commercially available thiazole-2-amines **2l-2n** [37].(See Table 4)

Compounds **8b-8v** and **9a-9g** were prepared as shown in Scheme 2. The starting materials of substituted benzylamines **3** were reacted with CDI to produce the corresponding intermediates **6b-6v** and **7a-7g**, which were then reacted with compound **2f** to give the final compounds **8b-8v** and **9a-9g**, respectively.

As shown in Scheme 3, the synthetic intermediates **2h-2m** were obtained by the reaction of compounds **1h-1m** with malononitrile in the presence of sulfur. 2,4-Dimethoxybenzylamine **3r** was reacted with CDI to produce intermediate **6r**, which was then reacted with **2h-2m** to afford the thiophen-urea derivatives **10a-10f**. All of the ^{1}H and ^{13}C NMR, and HRESIMS spectra of target compounds can be found in Supplementary Material.

2.2. α-Glucosidase inhibition assay and SAR study

The α-glucosidase inhibitory activity of all the target compounds was tested by *in vitro* enzyme assay, with acarbose as the positive control. The inhibition rates of tested compounds at 100 μM and IC_{50} values for compounds with >50% inhibition at 100 μM were measured and displayed in Table 1. The first round of structural modification towards hit **5a** concerned the replacement of cyclohexyl by other ring systems, such as methyl cyclohexyl (**5b**), pyrazyl (**5c**), and 1-methylpiperidinyl (**5d**), to explore its effect on the activity. However, the results showed that none of these three analogues was active towards α-glucosidase.

Then the replacement of carboxylate group with cyano group in the second round led to the production of **5e-5k** possessing different ring systems fused with thiophen. Interestingly, compared with **5a**, a more potent compound **5f** (IC_{50} of 10.18 ± 0.28 μM) was found, suggesting that the moiety of 3-cyano-4,5,6,7-tetrahydrobenzo[*b*]thiophenol core was favorable for the inhibitory activity, and especially, the cyclohexyl played a critical role in the activity since other ring systems connected to thiophenol made the activity of compounds (**5e**, **5g-5j**, and **5k**) diminished. During the third round of optimization, three analogues **5l-5n** were prepared by using thiazole to replace the thiophenol ring. However, these compounds did not exhibit activity towards α-glucosidase, with low inhibition rate of 26.43%~2.02% at 100 μM. Therefore, based on these preliminary results, it was deduced that the 3-cyano-4,5,6,7-tetrahydrobenzo[*b*]thiophenol moiety was a key fragment for the α-glucosidase inhibitory activity.

In the subsequent round, the 3-cyano-4,5,6,7-tetrahydrobenzo[*b*]thiophenol moiety was conserved, and different substituents were introduced to the benzene ring, resulting into the production of analogues **8b-8v**. From the results in Table 2, it was observed that most of compounds in this series showed improved activity compared to **5f**. Several compounds, such as **8b**, and **8p-8s** containing the alkoxy group/s at benzene ring, have lower IC_{50} values (1.67 ± 0.08 to 0.59 ± 0.02 μM), indicating that methoxyphenyl and ethoxyphenyl were key pharmacophores. Whereas the introduction of the bulky phenyl groups (**8t-**

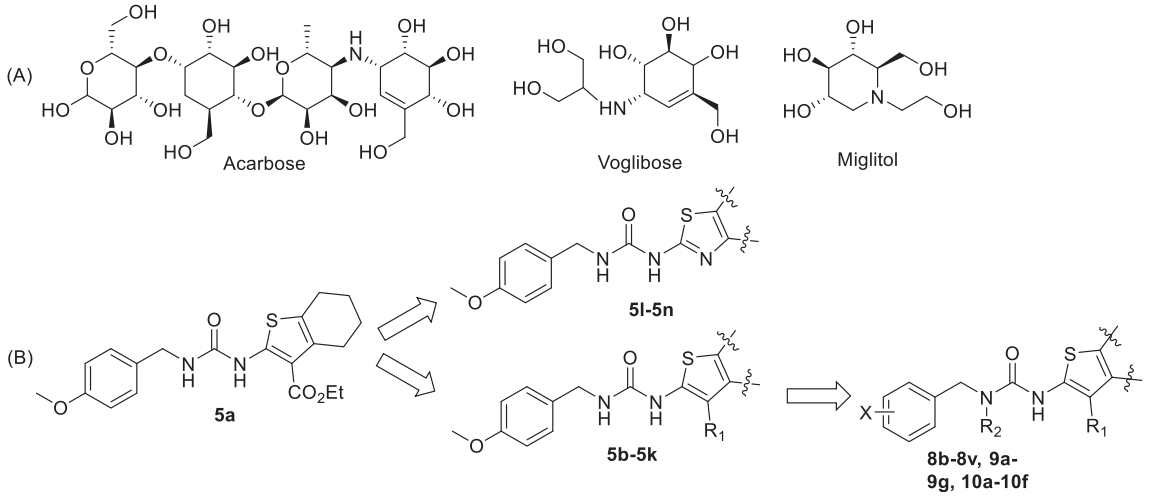

Fig. 1. Approved α-glucosidase inhibitors (A), and the α-glucosidase inhibitors (B) reported in this study.

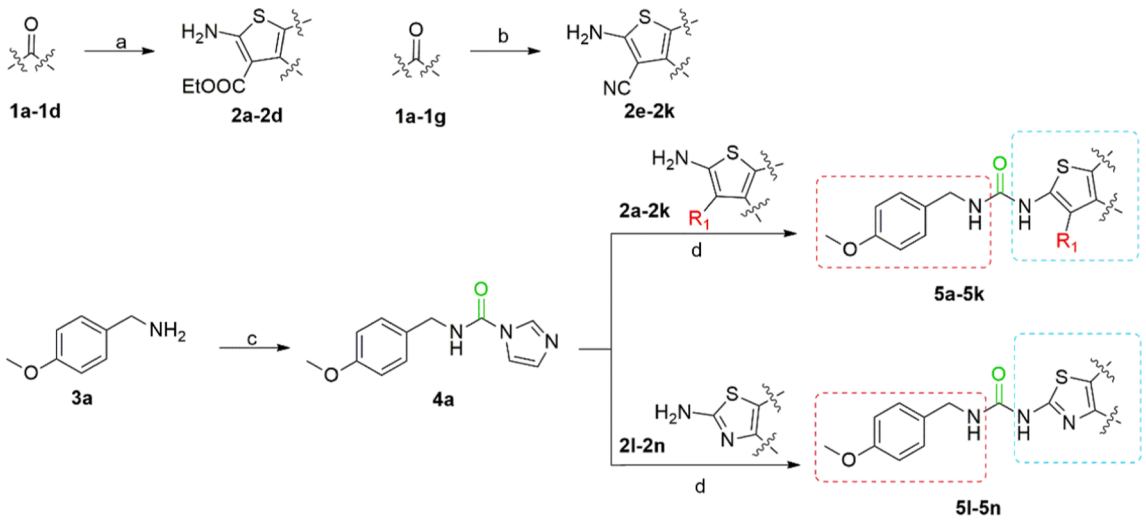

Scheme 1. Synthesis of compounds **2a-2k** and **5a-5n**. Reagents and conditions: (a) S_8, Morpholine, EtOH, 60 ℃, 4–7 h; (b) S_8, $NaAlO_2$, EtOH, 60 ℃, 4–7 h; (c) CDI, isopropyl alcohol hydrochloride, DMF, DCM, rt., 3–4 h; (d) NaH, DCM, r.t., 8–10 h.

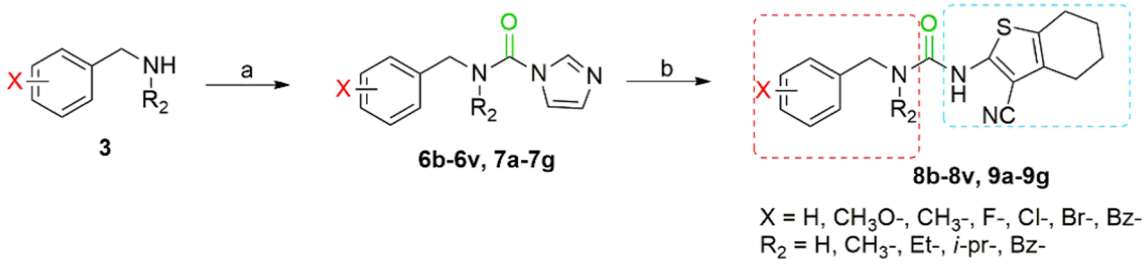

Scheme 2. Synthesis of compounds **8b-8v** and **9a-9g**. Reagents and conditions: (a) CDI, isopropyl alcohol hydrochloride, DMF, DCM, r.t., 3–4 h; (b) **2f**, NaH, DCM, r. t., 8–10 h.

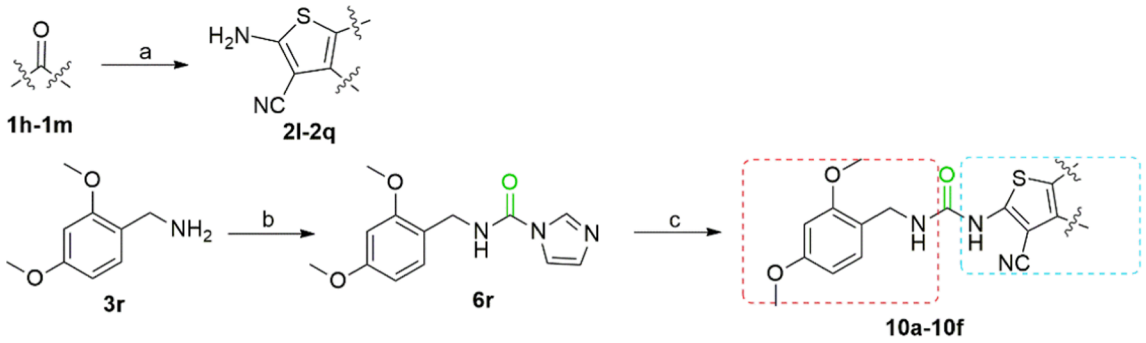

Scheme 3. Synthesis of compounds **2l-2q** and **10a-10f**. Reagents and conditions: (a) S_8, Morpholine, EtOH, 60 ℃, 4–7 h; (b) CDI, isopropyl alcohol hydrochloride, DMF, DCM, r.t., 3–4 h; (c) **2l-2q**, NaH, DCM, rt., 8–10 h.

8v) led to the significant decrease or loss of activity, which probably be attributed to the steric effect of naphthyl. In the meantime, another series of analogues **9a-9g** with substituents at *N* atom of urea was obtained, however only one compound **9a** showed decreased inhibitory activity with an IC_{50} value of 4.81 ± 0.09 μM.

In the final round of structural modification, several ring systems having more structural diversity were fused into the thiophene on basis of the most potent inhibitor **8r** to produce analogues **10a-10f**, in which the meta-dimethoxyphenyl fragment was conserved since it made the activity improve significantly. However, the activity of all these compounds was decreased or completely lost. The results of bioassay were shown in Table 3.

*2.3. α-Amylase inhibition assay of compounds **8r** and **8s***

Next, the inhibitory activities of **8r** and **8s** against α-amylase were evaluated with acarbose as a reference. As shown in Fig. 4, the comparison of their IC_{50} values indicated that compounds **8r** and **8s** exhibited high selectivity towards α-glucosidase over α-amylase by 51- and 86-fold. Selective inhibition against α-glucosidase over α-amylase is important because it could allow the hydrolysis of polysaccharides into oligosaccharides catalyzed by α-amylases to avoid the side effects of drugs as mentioned above [15,16].

Table 1
Inhibitory activity of **5a-5n** against α-glucosidase.

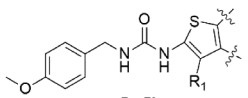

5a-5k

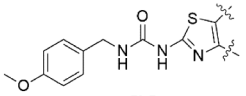

5l-5n

Compound	R_1	Group	Inhibition at 100 μM (%)	IC_{50} (μM)[a]
5a	-CO_2Et		87.76	26.71 ± 1.80
5b	-CO_2Et		22.71	-[b]
5c	-CO_2Et		24.54	–
5d	-CO_2Et		4.06	–
5e	-CN		49.04	–
5f	-CN		73.02	10.18 ± 0.28
5g	-CN		52.80	–
5h	-CN		39.15	–
5i	-CN		9.46	–
5j	-CN		−0.17	–
5k	-CN		67.35	43.53 ± 1.18
5l		5-NO_2	26.43	–
5m			12.10	–
5n			2.02	–
Acarbose				258.53 ± 1.27

[a] IC_{50} value was expressed as mean ± SD from three independent experiments.
[b] IC_{50} value was not tested if inhibition rate was <50% at 100 μM.

2.4. Compounds **8r** and **8s** quenched the intrinsic fluorescence of α-glucosidase

The direct interactions of **8r** and **8s** with α-glucosidase were confirmed by performing a fluorescence quenching experiment. As shown in Fig. 2, α-glucosidase exhibited an intrinsic fluorescence emission peak at 335 after being excited at a wavelength of 290 nm. After treatment with increasing concentrations of compounds **8r** (Fig. 2A) or **8s** (Fig. 2B), the intrinsic fluorescence emission of α-glucosidase was gradually quenched in a concentration-dependent manner, which thus confirmed the interactions of **8r** and **8s** with α-glucosidase.

2.5. Kinetic study of **8r** and **8s** on enzyme inhibition

To further probe the inhibition mechanism of tetrahydrobenzo[*b*]thiophen-2-yl)urea derivatives on α-glucosidase, an inhibition kinetics study was performed. The inhibition types of the most potent compounds **8r** and **8s**, based on their IC_{50} values, were tested using Lineweaver-Burk plot analysis. As shown in Fig. 3A, the double reciprocal plots at different concentrations of substrate had the same Michaelis constant (K_m), while the V_{max} decreased with decreasing concentration of **8r** and **8s**. This behavior indicated that both compounds were non-competitive inhibitors for α-glucosidase [39,40]. In addition, as shown in Fig. 3B, the plot of the slop against the concentration of **8r** and **8s** provided the steady-state inhibition constant (K_i), the values of which was estimated to be 8.6 μM (**8r**) and 6.2 μM (**8s**), respectively.

2.6. Homology modelling and molecular docking

Homology modelling was used to construct the 3-D structure of α-glucosidase (*Saccharomyces cerevisiae* organism, EC:3.2.1.20) with the online program SWISS MODEL (https://swissmodel.expasy.org/). Template search result (Table 5) indicated that 3AJ7 was the better template compared with 3AXH [10]. Therefore, 3AJ7 was selected as the template to construct the 3-D structure of α-glucosidase. To validate the stability of 3-D structure of α-glucosidase, 2 ns molecular dynamics simulation was performed. As illustrated in Fig. S1 (ESI†), the stable root-mean-square deviation (RMSD) values for backbone atoms of the α-glucosidase indicated that the modeled structure was reliable.

Molecular docking simulation was performed to probe the binding modes of compounds **8r** and **8s** with α-glucosidase. As shown in Table 6, both of the two compounds displayed higher docking scores when they were docked to the allosteric site compared to the active site. The two possible binding modes (the allosteric site and the active site) of **8r** and **8s** were shown in Fig. 4, respectively. These docking results were consistent with the noncompetitive property of these two compounds validated in the enzyme kinetic assay. The detailed interactions between the two compounds (**8r** and **8s**) with α-glucosidase (allosteric site) were shown in Fig. 5. It was seen that the hydrogen bonds, hydrophobic and the π-π stacking interactions were the main interactions that contributed to the binding affinity of inhibitors with the enzyme. The Fig. S2 (ESI†) of the detailed ligand protein interactions showed that **8r** established two hydrogen bonds with Asn412 and Lys155 residues, and formed hydrophobic interactions with Phe157, Gly159, Thr234, Ser235, Leu237, His239, Glu304, Phe311, Arg312, Ile415, Phe420 residues, and **8s** formed three hydrogen bonds with Asn241, Trp242, Pro309 residues, and established hydrophobic interactions with Phe157, Phe231, His239, Phe310, Phe311, Arg312, His279 residues. From these results of the docking simulation, it can be found that **8r** and **8s** bind to allosteric sites away from the active site (D214, E276 and D349) of the enzyme. Together, all of the data indicated that compounds **8r** and **8s** were noncompetitive inhibitor of α-glucosidase.

2.7. Druglikeness property prediction

Discovery studio 3.0 and online molinspiration were used to predict the druglikeness properties of **8r** and **8s**. From the results in Table 7, the chemical properties of two compounds fell into the Lipinski's "Rule of five", and were predicted to have acceptable solubility and absorption level. Importantly, both of them may not bind to PPB and CYP2D6, which possibly indicated fewer side effects of this series of compounds.

2.8. In vitro cytotoxicity

Due to that the liver is the primary organ responsible for drug metabolism, the effects of compounds **8r** and **8s** on the growth of human normal hepatocyte (LO2) and human liver cancer (HepG2) cells were evaluated using the MTT method, with acarbose as negative control and doxorubicin as positive control [41]. As shown in Fig. 6 and Table 8, the cell viability of LO2 cells treated with 100 μM acarbose, **8r**, and **8s** were 100.4 ± 4.0%, 94.7 ± 2.4%, and 95.5 ± 1.8%, respectively, and the cell viability of HepG2 cells treated with 100 μM acarbose, **8r**, and **8s** were 95.2 ± 2.3%, 96.3 ± 2.5%, and 96.0 ± 1.6%, respectively, indicating

Table 2
Inhibitory activities of **8b-8v** and **9a-9g** against α-glucosidase.

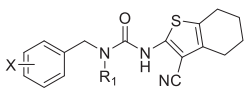

8b-8s,8v
9a-9f

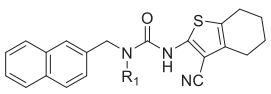

8t

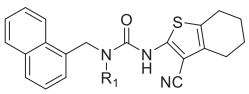

8u, 9g

Compound	X	R_1	Inhibition at 100 μM (%)	IC_{50}(μM)[a]
8b	2-OCH_3	H	91.64	1.67 ± 0.08
8c	3-OCH_3	H	79.46	0.77 ± 0.03
8d	H	H	64.59	63.11 ± 0.05
8e	2-CH_3	H	49.38	-[b]
8f	3-CH_3	H	68.75	12.61 ± 0.86
8g	4-CH_3	H	51.34	–
8h	4-F	H	37.38	–
8i	2-Cl	H	89.14	16.53 ± 1.05
8j	3-Cl	H	76.54	31.23 ± 1.03
8k	4-Cl	H	75.49	34.55 ± 1.48
8l	2-Br	H	70.28	9.08 ± 0.09
8m	3-Br	H	84.54	16.19 ± 0.87
8n	4-Br	H	42.29	–
8o	4-OC_2H_5	H	71.24	22.18 ± 1.52
8p	2-OC_2H_5	H	81.37	0.96 ± 0.04
8q	3,4-OCH_3	H	89.57	1.41 ± 0.09
8r	2,4-OCH_3	H	88.58	0.59 ± 0.02
8s	3,5-OCH_3	H	91.12	0.65 ± 0.03
8t		H	53.51	89.67 ± 0.79
8u		H	36.22	–
8v	4-Ph	H	13.62	–
9a	H	-CH_3	77.83	4.81 ± 0.09
9b	2-CH_3	-CH_3	21.24	–
9c	4-CH_3	-CH_3	19.28	–
9d	H	-Et	8.15	–
9e	H	-i-pr	14.78	–
9f	H	-Bz	4.51	–
9g		-CH_3	8.88	–

[a] IC_{50} value was expressed as mean ± SD from three independent experiments.
[b] IC_{50} value was not tested if inhibition rate was <50% at 100 μM.

Table 3
Inhibitory activities of **10a-10f** against α-glucosidase.

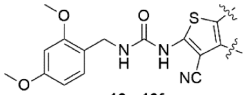

10a-10f

Compound	Group	Inhibition rate at 100 μM (%)	IC_{50} (μM)[a]
10a	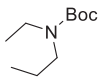	36.20	-[b]
10b		75.42	7.17 ± 0.26
10c		9.14	–
10d		26.14	–
10e	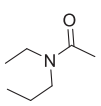	4.80	–
10f	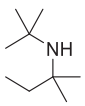	13.95	–

[a] IC_{50} value was expressed as mean ± SD from three independent experiments.
[b] IC_{50} value was not tested if inhibition rate was<50% at 100 μM.

Table 4
Inhibitory activities of **8r** and **8s** against α-amylase.

Compounds	IC_{50} (μM)		Index[a]
	α-glucosidase	α-amylase	
8r	0.59 ± 0.02	30.37 ± 0.58	51
8s	0.65 ± 0.03	56.14 ± 0.71	86
Acarbose	258.53 ± 1.27	70.82 ± 0.89	0.27

[a] IC_{50} (α-amylase)/IC_{50} (α-glucosidase).

that both compounds did not affect on the growth of LO2 and HepG2 cells. The results disclosed that **8r** and **8s** had CC_{50} values >100 μM. To be a potential drug, the ratio of CC_{50}/IC_{50} (SI) should be equal or great than 10. In the case of **8r** and **8s**, their SI values are much >150 indicating that they are non-cytotoxic towards LO2 and HepG2 cell lines and have selectivity towards the enzyme inhibition [18].

2.9. *In vivo anti-hyperglycemic effects of **8r** and **8s***

The antihyperglycemic effects of compounds **8r** and **8s** on normal rats were evaluated, with acarbose as a positive control. As shown in Fig. 7A, the level of the control group increased rapidly after sucrose treatment (81.00 ± 6.69 mg/dL at 0 min vs 183.45 ± 23.41 mmol/L at 20 min), and the glucose load basically reached the highest level at 30 min after sucrose treatment. In the administration groups, the levels of blood glucose of rats treated with compounds **8r**, **8s** or acarbose were lower than that of control group, and especially it began to decrease after 45 min. Thus, it could be concluded that they had significant hypoglycemic effects. The results in Fig. 7B revealed that the areas under

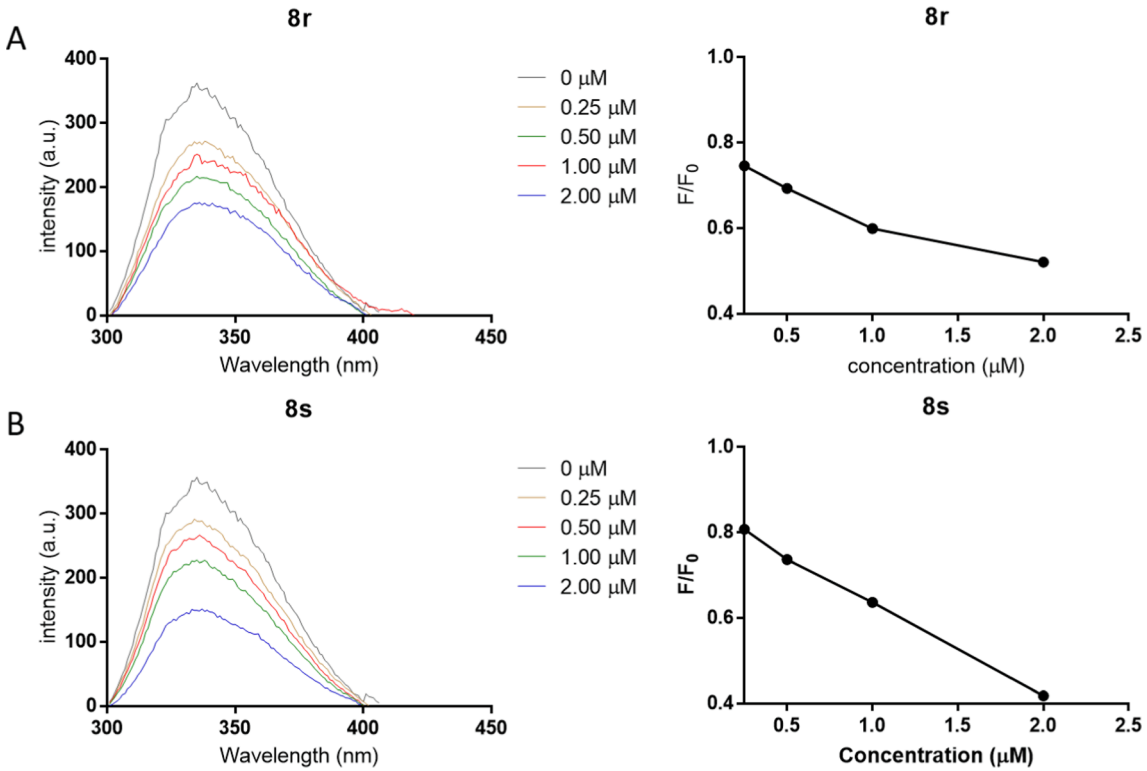

Fig. 2. Variation of fluorescence emission spectra of α-glucosidase (1U/mL) without or in the presence of **8r** (A) and **8s** (B). The intrinsic fluorescence emission peak of α-glucosidase was observed at 335 nm after being excited at 290 nm (left graph), and compounds **8r** and **8s** quenched the intrinsic fluorescence of enzyme in a concentration-dependent manner (right graph).

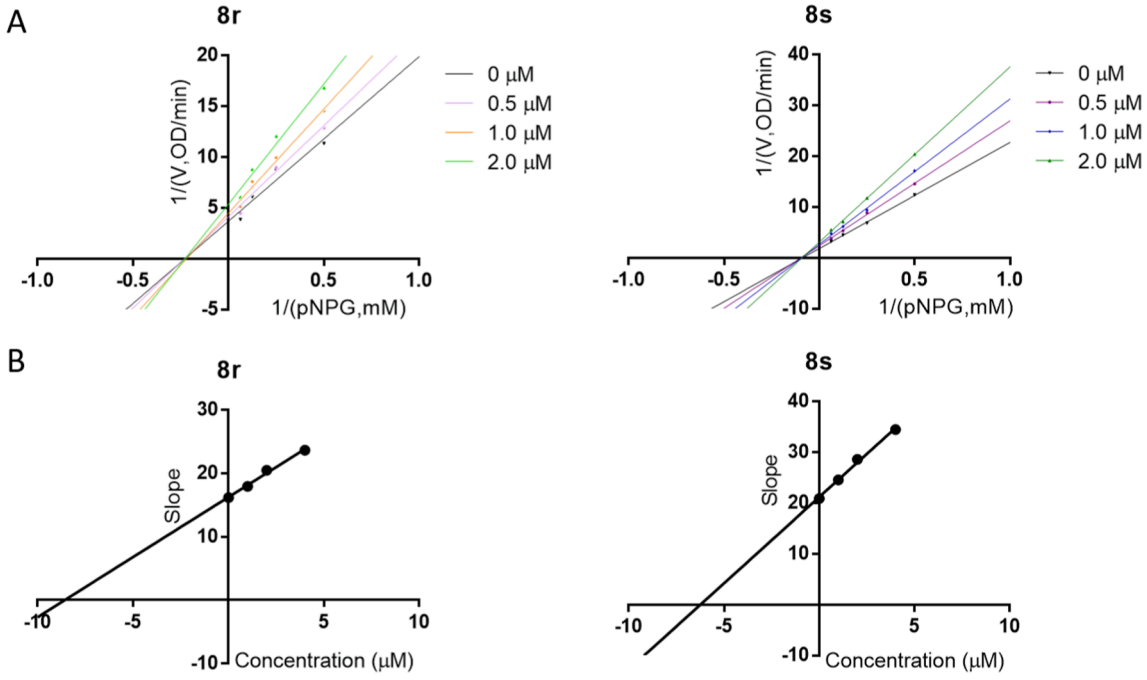

Fig. 3. Kinetic analysis of compounds **8r** and **8s** interacting with α-glucosidase. A: Lineweaver-Burk reciprocal plots of initial velocity and increasing substrate (pNPG) concentration; B: the secondary plot of slopes versus the concentration of inhibitors.

the blood glucose curve (AUC) of the administration groups of **8r** and acarbose significantly decreased in 2 h vs control group, which indicated that compound **8r** could improve the oral sucrose tolerance. All these results indicated that compound **8r** could improve sucrose tolerance *in vivo* and suppress the postprandial hyperglycemia by inhibiting α-glucosidase.

3. Conclusion

In summary, a new tetrahydrobenzo[*b*]thiophen-2-yl)urea-based

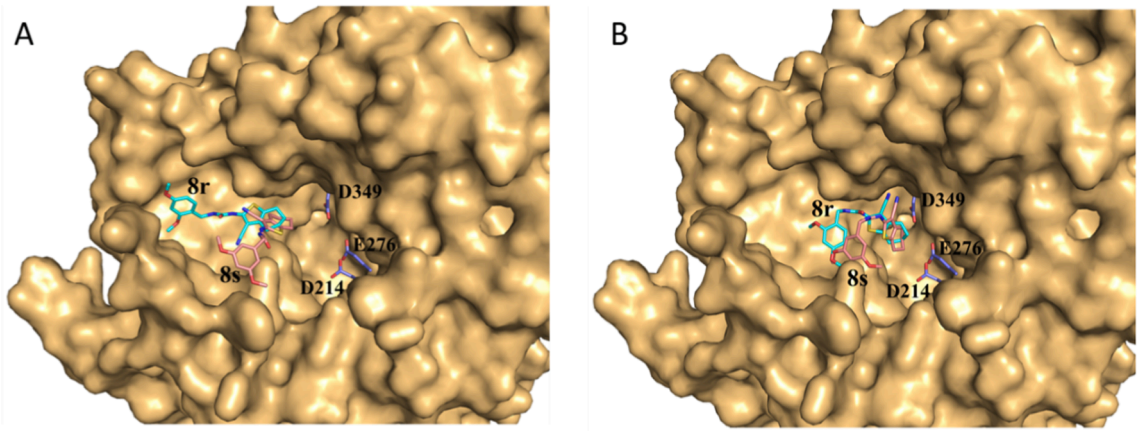

Fig. 4. The proposed binding modes of compounds **8r**, and **8s** with α-glucosidase (A: allosteric site; B: active site). The α-glucosidase and compounds were shown as surface and sticks, respectively. Residues in the active site (D214, E276 and D349) were also shown as sticks.

Table 5
Template search results.

Template	Seq Identity	Resolution	Seq Similarity	GMQE	QMEAN
3AJ7	72.68	1.30 Å	0.55	0.94	0.08
3AXH	72.51	1.80 Å	0.55	0.94	0.17

Table 6
Molecular docking score results.

Compounds	Docking score (Allosteric site)	Docking score (Active site)
8r	−4.665	−4.389
8s	−5.503	−3.832

α-glucosidase inhibitor **5a** was identified from our in-house compound library, and then a series of its analogues were synthesized and evaluated for their α-glucosidase inhibitory activities. In addition, their inhibition types and binding with α-glucosidase were explored by kinetic study, fluorescence quenching experiments, and molecular docking. Finally, their *in vitro* cytotoxicities and *in vivo* anti-hyperglycaemic effects were evaluated.

Among all the analogues, most of series of compounds **8**, possessing 1-benzyl-3-(3-cyano-4,5,6,7-tetrahydrobenzo[*b*]thiophen-2-yl)urea framework, displayed promising α-glucosidase inhibitory activity, with compounds **8r** and **8s** being the most potent inhibitors with IC_{50} values of 0.96 ± 0.04 and 0.59 ± 0.02 μM, respectively. The SAR analysis suggested that ring systems fused with a thiophenyl core could significantly affect the activity of compounds, and a cyano group in the thiophene and alkoxyl groups one the benzene could improve the α-glucosidase inhibitory activity. In addition, the replacement of thiophene by thiazole resulted in completely loss of activity. Molecular docking studies revealed that the increase of the activities could be attributed to hydrogen bonds, hydrophobic and the π-π stacking interactions of compounds with the α-glucosidase enzyme. The binding of the most potent compounds **8r** and **8s** towards α-glucosidase was confirmed by fluorescence quenching experiments. Further kinetics study suggested that both compounds inhibited α-glucosidase via a

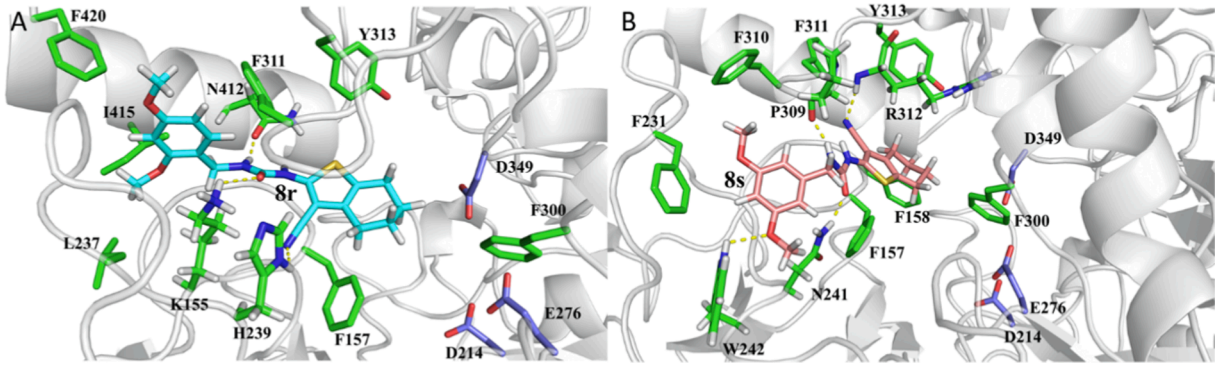

Fig. 5. The detailed ligand–protein interactions established between **8s** (A)/**8s** (B) and allosteric site of α-glucosidase. The yellow dashed lines represent hydrogen bonds, and residues involved in the hydrophobic and the π-π stacking interactions were labeled and shown as sticks. (For interpretation of the references to colour in this figure legend, the reader is referred to the web version of this article.)

Table 7
Prediction of druglikeness properties of **8r** and **8s**.

No.	MW	No. HBA	No. HBD	cLogP	No. Rotatable bond	Solubility level	Absorption level	PPB	CYP2D6
8r	372	6	2	3.53	5	2	0	2.08196	FALSE
8s	372	6	2	3.732		2	0	1.18478	FALSE

MW < 500; No. HBA < 10; No. HBD < 5; cLogp < 5; No. Rotatable bond < 10; Solubility Level: (0, Good; 1, Moderate; 2, Poor; 3, Very poor); Absorption Level: (0, Good; 1, Moderate; 2, Poor; 3, Very poor); PPB: plasma protein binding; CYP2D6: Cytochrome P450 2D6 inhibition.

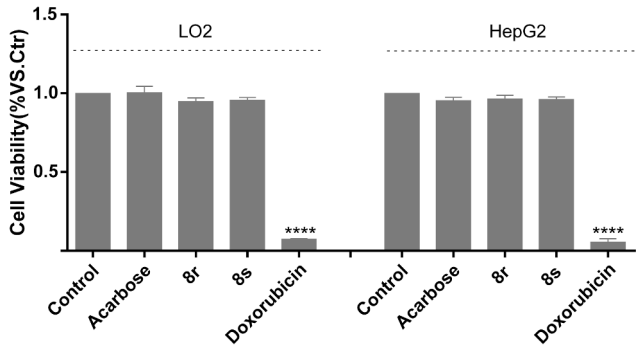

Fig. 6. Effects of compounds **8r**, **8s**, acarbose, and doxorubicin at 100 μM on the cell viability of LO2 and HepG2 cell lines. Data are expressed as mean ± SD (n = 3), and ****P < 0.0001versus control group.

Table 8
The CC_{50} values of **8r** and **8s** towards LO2 and HepG2 cell lines

Compounds	CC_{50} (μM)	
	LO2	HepG2
8r	>100	>100
8s	>100	>100
Acarbose	>100	>100
Doxorubicin	2.50 ± 0.08	1.32 ± 0.12

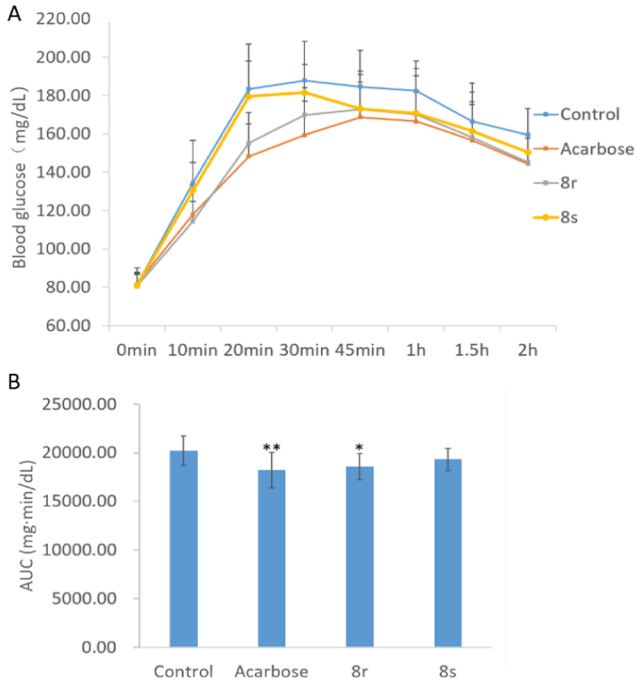

Fig. 7. The effects of compounds **8r** and **8s** on the glucose level in normal rat model. The SD rats were treated with or without 5 mg/kg tested compounds, and then 7.5 g/kg sucrose solutions 30 min after oral administration, and the glucose level was tested at 0–2 h. Data are mean ± SD, n = 12. *P < 0.05 and **P < 0.001.

noncompetitive mechanism, which is consistent with the molecular docking results that these compounds were more likely to bind to an allosteric site rather than the active site of α-glucosidase.

The results of *in vitro* cytotoxicity bioassay showed that compounds **8r** and **8s** had no significant effect on the growth of HepG2 and LO2 cells even at 100 μM. Most importantly, compound **8r** was demonstrated to lower glucose levels in SD rats at a dose of 5 mg/kg, and to have a comparable anti-hyperglycemic activity with acarbose. As a result, these compounds may be promising lead compounds for developing novel α-glucosidase inhibitors used in type 2 diabetes treatment.

4. Materials and methods

4.1. General

The α-glucosidase of *Saccharomyces cerevisiae* (EC 3.2.1.20), porcine pancreatic α-amylase (EC 3.2.1.1), and substrate pNPG (N1377) were purchased from Sigma-Aldrich. All other commercially available reagents were used without further purification. Organic solvents were evaporated with reduced pressure using a Büchi R-100 evaporator. Reactions were monitored by TLC using Yantai Jingyou (China) GF254 silica gel plates. Silica gel column chromatography was performed on silica gel (200–300 mesh) from Qingdao Hailang (China). NMR spectra were measured on Bruker Avance III 600 MHz spectrometers. Chemical shifts were expressed in δ (ppm) and coupling constants (J) in Hz with solvent signals as internal standards ($CDCl_3$, δ_H 7.26 ppm and δ_C 77.2 ppm; DMSO-d_6, δ_H 2.50 ppm and δ_C 39.5 ppm). ESI-MS analyses were performed on an Agilent 1260–6460 Triple Quard LC-MS instrument (Agilent, Waldbronn, Germany), and HR-ESI-MS data were acquired on an Agilent Q-TOF 6520. Medium M199 and bovine serum were obtained from Gibco Co. (Carlsbad, CA, USA).

4.2. Synthesis of compounds

4.2.1. Synthesis of compounds ***2a~2k***

General method A:To a solution of cyclic ketone compounds in anhydrous ethanol (conc. 0.1 M) was added sodium (6 % mmol), sulfur (1.1 eq) and malononitrile (1 eq) or ethyl cyanoacetate (1 eq) at 60 °C. The reaction mixture was stirred for 4–7 h. After the completion of the reaction, the reaction solution was concentrated and purified by flash column chromatography with solution of EtOAc/petroleum ether to obtain compounds.

*4.2.1.1. Ethyl 2-amino-4,5,6,7-tetrahydrobenzo[b]thiophene-3-carboxylate **(2a)**.* Rf = 0.30 (EtOAc/petroleum ether = 1/15), ^{1}H NMR (600 MHz, DMSO-d_6) δ 7.19 (s, 2H), 4.14 (q, J = 7.1 Hz, 2H), 2.59 (t, J = 5.7 Hz, 2H), 2.41 (t, J = 5.7 Hz, 2H), 1.72–1.60 (m, 4H), 1.23 (t, J = 7.1 Hz, 3H). ^{13}C NMR (150 MHz, DMSO-d_6) δ 165.1, 162.9, 131.3, 115.5, 102.6, 58.6, 39.5, 26.5, 23.9, 22.8, 22.4, 14.4.

*4.2.1.2. Ethyl 2-amino-6-methyl-4,5,6,7-tetrahydrobenzo[b]thiophene-3-carboxylate **(2b)**.* Rf = 0.30 (EtOAc/petroleum ether = 1/20), ^{1}H NMR (600 MHz, $CDCl_3$) δ 5.92 (s, 2H), 4.25 (q, J = 7.1 Hz, 2H), 2.91–2.83 (m, 1H), 2.63–2.56 (m, 1H), 2.56–2.52 (m, 1H), 2.13 (m, 1H), 1.90–1.79 (m, 2H), 1.33 (t, J = 7.1 Hz, 4H), 1.04 (d, J = 6.5 Hz, 3H). ^{13}C NMR (150 MHz, $CDCl_3$) δ 166.3, 161.9, 132.2, 117.4, 105.8, 59.5, 32.8, 31.3, 29.6, 26.9, 21.6, 14.6.

*4.2.1.3. Ethyl 2-amino-4,7-dihydro-5H-thieno[2,3-c]pyran-3-carboxylate **(2c)**.* Rf = 0.30 (EtOAc/petroleum ether = 1/6), ^{1}H NMR (600 MHz, $CDCl_3$) δ 6.00 (s, 2H), 4.55 (s, 2H), 4.26 (q, J = 7.1 Hz, 2H), 3.90 (t, J = 5.6 Hz, 2H), 2.82 (tt, J = 5.6, 2.0 Hz, 2H), 1.33 (t, J = 7.1 Hz, 3H). ^{13}C NMR (150 MHz, $CDCl_3$) δ 166.0, 162.3, 130.4, 114.9, 105.6, 65.3, 64.7, 59.7, 27.8, 14.6.

*4.2.1.4. Ethyl 2-amino-6-methyl-4,5,6,7-tetrahydrothieno[2,3-c]pyridine-3-carboxylate **(2d)**.* Rf = 0.32 (EtOAc/petroleum ether = 1/6), ^{1}H NMR (600 MHz, $CDCl_3$) δ 6.00 (s, 2H), 4.25 (q, J = 7.1 Hz, 2H), 3.36 (q, J = 1.7 Hz, 2H), 2.83 (t, J = 5.9 Hz, 2H), 2.65 (t, J = 5.9 Hz, 2H), 2.43 (s, 3H), 1.32 (t, J = 7.1 Hz, 3H). ^{13}C NMR (150 MHz, $CDCl_3$) δ 166.1, 162.2, 130.8, 114.7, 105.5, 59.6, 53.4, 52.6, 45.6, 27.5, 14.6.

*4.2.1.5. 2-Amino-5,6-dihydro-4H-cyclopenta[b]thiophene-3-carbonitrile (**2e**).* Rf = 0.40 (EtOAc/petroleum ether = 1/6), ^{1}H NMR (600 MHz, $CDCl_3$) δ 4.64 (s, 2H), 2.78–2.73 (m, 2H), 2.73–2.67 (m, 2H), 2.36 (p, J = 7.1 Hz, 2H). ^{13}C NMR (150 MHz, $CDCl_3$) δ 165.4, 142.1, 125.3, 115.7, 84.8, 29.4, 28.6, 27.5.

*4.2.1.6. 2-Amino-4,5,6,7-tetrahydrobenzo[b]thiophene-3-carbonitrile (**2f**).* Rf = 0.30 (EtOAc/petroleum ether = 1/6), ^{1}H NMR (600 MHz, $CDCl_3$) δ 4.68 (s, 2H), 2.53–2.42 (m, 4H), 1.78 (m, 4H). ^{13}C NMR (150 MHz, $CDCl_3$) δ 160.2, 132.4, 120.6, 115.7, 88.6, 24.6, 24.2, 23.4, 22.2.

*4.2.1.7. 2-Amino-5,6,7,8-tetrahydro-4H-cyclohepta[b]thiophene-3-carbonitrile (**2g**).* Rf = 0.30 (EtOAc/petroleum ether = 1/6), ^{1}H NMR (600 MHz, $CDCl_3$) δ 2.82–2.74 (m, 2H), 2.47–2.43 (m, 2H), 1.74 (dt, J = 9.5, 4.4 Hz, 2H), 1.70–1.66 (m, 2H), 1.57 (dt, J = 5.7, 2.7 Hz, 2H). ^{13}C NMR (150 MHz, $CDCl_3$) δ 215.4, 111.9, 43.9, 36.3, 30.4, 29.0, 26.2, 24.3.

*4.2.1.8. 2-Amino-4-methyl-4,5,6,7-tetrahydrobenzo[b]thiophene-3-carbonitrile (**2i**).* Rf = 0.25 (EtOAc/petroleum ether = 1/5),^{1}H NMR (600 MHz, $CDCl_3$) δ 4.67 (s, 2H), 2.80 (m, 1H), 2.52–2.44 (m, 2H), 1.87–1.80 (m, 2H), 1.78–1.74 (m, 1H), 1.59–1.52 (m, 1H), 1.26 (d, J = 7.1 Hz, 3H). ^{13}C NMR (151 MHz, $CDCl_3$) δ 160.5, 137.1, 120.5, 115.9, 86.3, 30.2, 29.4, 24.4, 20.6, 19.9.

*4.2.1.9. 2-Amino-4,7-dihydro-5H-thieno[2,3-c]pyran-3-carbonitrile (**2J**).* Rf = 0.25 (EtOAc/petroleum ether = 1/4), ^{1}H NMR (600 MHz, DMSO-d_6) δ 7.11 (s, 2H), 4.41 (d, J = 2.1 Hz, 2H), 3.82 (t, J = 5.5 Hz, 2H), 2.48–2.35 (m, 2H). ^{13}C NMR (150 MHz, DMSO-d_6) δ 164.0, 129.6, 116.3, 114.9, 83.2, 64.2, 64.1, 25.0.

*4.2.1.10. 2-Amino-6-methyl-4,5,6,7-tetrahydrothieno[2,3-c]pyridine-3-carbonitrile (**2k**).* Rf = 0.50 (Acetone/petroleum ether = 2.5/1), ^{1}H NMR (600 MHz, DMSO-d_6) δ 7.03 (s, 2H), 3.23 (d, J = 2.1 Hz, 2H), 2.58 (t, J = 5.7 Hz, 2H), 2.42 (td, J = 5.7, 2.8 Hz, 2H), 2.31 (s, 3H). ^{13}C NMR (150 MHz, DMSO-d_6) δ 163.7, 130.0, 116.5, 114.9, 83.2, 52.7, 51.6, 45.3, 24.8.

*4.2.2. Synthesis of compounds **4a***

General method B: To a solution of benzylamine derivatives in anhydrous DCM (conc. 0.3 M) was slowly added a solution of hydrochloric acid in isopropanol with stirring until it becomes thick white turbid liquid at room temperature. Then CDI (5.6 mmol) in DMF (6 ml) solution was added dropwise. The reaction mixture was stirred for 3–4 h at room temperature under argon then was diluted with AcOEt and brine. The aqueous layer was extracted with AcOEt and the combined organic extracts were washed with brine, dried over Na_2SO_4 and concentrated under vacuum. The precipitate was washed with Et_2O to give the desired *N*-(4-methoxybenzyl)-1H-imidazole-1-carboxamide (**4a**) as a colored solid. White solid; yield 81.2%; Rf = 0.20 (acetone/petroleum ether = 1/2), ^{1}H NMR (600 MHz, $CDCl_3$) δ 8.07 (s, 1H), 7.39 (t, J = 1.5 Hz, 1H), 7.24 (s, 2H), 6.93 (s, 1H), 6.87 (d, J = 8.6 Hz, 2H), 4.50 (d, J = 5.5 Hz, 2H), 3.79 (s, 3H). ^{13}C NMR (150 MHz, $CDCl_3$) δ 159.5, 149.0, 135.9, 130.1, 129.6, 129.2, 116.4, 114.4, 55.5, 44.6.

*4.2.3. Synthesis of compounds **5a-5n***

General method C: To a solution of compound **4** or **6** in DMF was added compound **2** (1 eq) and NaH (1.2 eq). After stirring for 8–10 h at room temperature. The reaction mixture was diluted with AcOEt and brine. The aqueous layer was extracted with AcOEt, and the combined organic extracts were washed with brine, dried over Na_2SO_4 and concentrated under vacuum. The residue was purified by flash column chromatography to give the desired compound as a solid.

*4.2.3.1. Ethyl 2-(3-(4-methoxybenzyl)ureido)-5,6-dihydro-4H-cyclopenta[b]thiophene-3-carboxylate (**5a**).* White solid; yield 39.2%; m.p.: 107–108 ℃; Rf = 0.55 (EtOAc/petroleum ether = 1/3), ^{1}H NMR (600 MHz, $CDCl_3$) δ 10.33 (s, 1H), 7.24 (d, J = 8.6 Hz, 2H), 6.95 (d, J = 8.6 Hz, 2H), 5.38 (s, 1H), 4.42 (d, J = 5.6 Hz, 2H), 4.20 (q, J = 7.1 Hz, 2H), 3.79 (s, 3H), 2.75 (t, J = 5.8 Hz, 2H), 2.60 (t, J = 5.8 Hz, 2H), 1.76 (dd, J = 5.8, 2.2 Hz, 2H), 1.70 (dd, J = 5.8, 2.2 Hz, 2H)., 1.31 (t, J = 7.1 Hz, 3H). ^{13}C NMR (150 MHz, $CDCl_3$) δ 166.6, 159.2, 155.1, 153.5, 141.0, 141.0, 130.3, 129.2, 114.2, 106.0, 60.3, 55.4, 44.3, 25.1, 23.9, 22.7, 21.7, 14.4. HRMS (ESI+): *m/z* calcd for $C_{20}H_{24}N_2O_4S^+$ $[M + H]^+$: 389.4820, found: 389.4863.

*4.2.3.2. Ethyl 2-(3-(4-methoxybenzyl)ureido)-6-methyl-4,5,6,7-tetrahydrobenzo[b]thiophene-3-carboxylate (**5b**).* Light yellow solid; yield 42.3%; m.p.: 99.5–101 ℃; Rf = 0.60 (EtOAc/petroleum ether = 1/3), ^{1}H NMR (600 MHz, $CDCl_3$) δ 10.64 (s, 1H), 7.24 (d, J = 8.6 Hz, 2H), 6.85 (d, J = 8.6 Hz, 2H), 5.27 (t, J = 5.0 Hz, 1H), 4.41 (d, J = 5.6 Hz, 2H), 4.26–4.19 (m, 2H), 3.79 (s, 3H), 2.88 (m, 1H), 2.69–2.58 (m, 2H), 2.24–2.19 (m, 1H), 1.89–1.81 (m, 2H), 1.33 (t, J = 7.1 Hz, 3H), 1.25 (d, J = 2.1 Hz, 1H), 1.05 (d, J = 6.5 Hz, 3H). ^{13}C NMR (150 MHz, $CDCl_3$) δ 167.2, 159.2, 153.6, 151.3, 130.2, 129.3, 124.8, 114.2, 114.1, 109.1, 60.3, 55.4, 53.6, 32.5, 31.4, 29.4, 26.4, 21.6, 14.4. HRMS (ESI+): *m/z* calcd for $C_{21}H_{26}N_2O_4^+$ $[M + H]^+$: 403.1692, found: 403.1713.

*4.2.3.3. Ethyl 2-(3-(4-methoxybenzyl)ureido)-4,7-dihydro-5H-thieno[2,3-c]pyran-3-carboxylate (**5c**).* White solid; yield 32.3%; m.p.: 130.5–131.5 ℃; Rf = 0.50 (EtOAc/petroleum ether = 1/2), ^{1}H NMR (600 MHz, $CDCl_3$) δ 10.60 (s, 1H), 7.24 (d, J = 8.4 Hz, 2H), 6.84 (d, J = 8.4 Hz, 2H), 5.53 (s, 1H), 4.64 (s, 2H), 4.41 (d, J = 5.6 Hz, 2H), 4.22 (q, J = 7.1 Hz, 2H), 3.91 (t, J = 5.6 Hz, 2H), 3.79 (d, J = 1.0 Hz, 3H), 2.83 (m, 2H), 1.32 (t, J = 7.1 Hz, 3H). ^{13}C NMR (150 MHz, $CDCl_3$) δ 166.7, 159.2, 153.5, 151.8, 129.2, 128.3, 122.6, 114.2, 108.8, 65.2, 64.8, 60.5, 55.4, 44.3, 27.2, 14.4. HRMS (ESI+): *m/z* calcd for $C_{19}H_{22}N_2O_5^+$ $[M + H]^+$: 391.1328, found: 391.1308.

*4.2.3.4. Ethyl 2-(3-(4-methoxybenzyl)ureido)-6-methyl-4,5,6,7-tetrahydrothieno[2,3-c]pyridine-3-carboxylate (**5d**).* Yellow solid; yield 34.7%; m.p.: 111–112 ℃; Rf = 0.40 (MeOH/CH_2Cl_2 = 5/95), ^{1}H NMR (600 MHz, $CDCl_3$) δ 10.56 (s, 1H), 7.24 (d, J = 8.6 Hz, 2H), 6.85 (d, J = 8.6 Hz, 2H), 5.52 (t, J = 5.6 Hz, 1H), 4.40 (d, J = 5.6 Hz, 2H), 4.22 (q, J = 7.1 Hz, 2H), 3.79 (s, 3H), 3.45 (s, 2H), 2.85 (m, 2H), 2.66 (t, J = 5.9 Hz, 2H), 2.44 (s, 3H), 1.32 (t, J = 7.1 Hz, 3H). ^{13}C NMR (150 MHz, $CDCl_3$) δ 166.8, 159.2, 153.5, 151.6, 129.2, 128.7, 122.3, 114.2, 108.7, 60.4, 55.4, 53.4, 52.6, 50.9, 45.7, 44.3, 27.1, 14.4. HRMS (ESI+): *m/z* calcd for $C_{20}H_{25}N_3O_4^+$ $[M + H]^+$: 404.1644, found: 404.1675.

*4.2.3.5. 1-(3-Cyano-5,6-dihydro-4H-cyclopenta[b]thiophen-2-yl)-3-(4-methoxybenzyl)urea (**5e**).* Light yellow solid; yield 73.5%; m.p.: 84–85.5 ℃; Rf = 0.25 (EtOAc/petroleum ether = 1/3), ^{1}H NMR (600 MHz, $CDCl_3$) δ 9.57 (s, 1H), 7.18 (d, J = 8.7 Hz, 2H), 6.79 (s, 1H), 6.78 (d, J = 8.7 Hz, 2H), 4.35 (d, J = 5.5 Hz, 2H), 3.73 (s, 3H), 2.77–2.74 (m, 2H), 2.68–2.65 (m, 2H), 2.35–2.30 (m, 2H). ^{13}C NMR (150 MHz, $CDCl_3$) δ 158.8, 155.9, 154.0, 140.2, 131.5, 130.9, 128.9, 115.6, 113.9, 85.2, 55.3, 43.5, 29.3, 28.1, 27.9. HRMS (ESI+): *m/z* calcd for $C_{17}H_{17}N_3O_2^+$ $[M + H]^+$: 328.1120, found: 328.1118.

*4.2.3.6. 1-(3-Cyano-4,5,6,7-tetrahydrobenzo[b]thiophen-2-yl)-3-(4-methoxybenzyl)urea (**5f**).* Light yellow solid; yield 79.1%; m.p.: 158–159 ℃; Rf = 0.30 (acetone/petroleum ether = 1/4),^{1}H NMR (600 MHz, $CDCl_3$) δ 8.69 (s, 1H), 7.22 (d, J = 8.6 Hz, 2H), 6.84 (d, J = 8.6 Hz, 2H), 6.04 (t, J = 5.6 Hz, 1H), 4.38 (d, J = 5.6 Hz, 2H), 3.78 (s, 3H), 2.55 (t, J = 5.9 Hz, 2H), 2.40 (t, J = 5.9 Hz, 2H), 1.81–1.76 (m, 4H). ^{13}C NMR (150 MHz, $CDCl_3$) δ 159.1, 153.7, 151.8, 130.4, 130.2, 129.0, 126.2, 116.2, 114.1, 89.2, 55.4, 43.9, 24.0, 24.0, 23.3, 22.3. HRMS (ESI+): *m/z* calcd for $C_{18}H_{19}N_3O_2^+$ $[M + H]^+$: 342.1276, found: 342.1227.

*4.2.3.7. 1-(3-Cyano-5,6,7,8-tetrahydro-4H-cyclohepta[b]thiophen-2-yl)-3-(4-methoxybenzyl)urea (**5g**).* White solid; yield 78.7%; m.p.: 225–226 ℃; Rf = 0.65 (EtOAc/petroleum ether = 1/4), ^{1}H NMR (600 MHz, $CDCl_3$) δ 8.47 (s, 1H), 7.24 (d, J = 8.6 Hz, 2H), 6.85 (d, J = 8.6 Hz, 2H), 5.89 (t, J = 5.5 Hz, 1H), 4.38 (d, J = 5.5 Hz, 2H), 3.78 (s, 3H), 2.64 (m, 2H), 2.54 (m, 2H), 1.83 (t, J = 5.6 Hz, 2H), 1.61 (d, J = 5.6 Hz, 2H), 1.25 (s, 2H). ^{13}C NMR (150 MHz, $CDCl_3$) δ 159.0, 153.6, 149.5, 134.7, 130.3, 129.7, 128.9, 116.4, 114.0, 91.8, 55.3, 43.8, 32.0, 29.0, 29.0, 28.1, 27.3. HRMS (ESI+): *m/z* calcd for $C_{19}H_{21}N_3O_2^+$ $[M + H]^+$: 356.1433, found: 356.1427.

*4.2.3.8. 1-(3-Cyano-6-methyl-4,5,6,7-tetrahydrobenzo[b]thiophen-2-yl)-3-(4-methoxybenzyl)urea (**5h**).* White solid; yield 69.8%; m.p.: 218.5–219.5 ℃; Rf = 0.90 (EtOAc/petroleum ether = 1/2), ^{1}H NMR (600 MHz, DMSO-d_6) δ 9.93 (s, 1H), 7.22 (d, J = 8.1 Hz, 2H), 7.10 (t, J = 5.8 Hz, 1H), 6.90 (d, J = 8.1 Hz, 2H), 4.25 (d, J = 5.8 Hz, 2H), 3.73 (s, 3H), 2.62 (dd, J = 16.0, 4.9 Hz, 1H), 2.47–2.41 (m, 1H), 2.12 (dd, J = 16.0, 9.6 Hz, 1H), 1.81 (d, J = 12.2 Hz, 2H), 1.34–1.32 (m, 1H), 1.23 (s, 1H), 1.01 (d, J = 6.5 Hz, 3H). ^{13}C NMR (150 MHz, DMSO-d_6) δ 158.8, 153.8, 150.9, 131.6, 129.9, 129.1, 125.0, 115.4, 114.3, 88.9, 55.5, 43.0, 31.8, 30.4, 29.6, 23.8, 21.6. HRMS (ESI+): *m/z* calcd for $C_{19}H_{21}N_3O_2^+$ $[M + H]^+$: 356.1433, found: 356.1413.

*4.2.3.9. 1-(3-Cyano-4-methyl-4,5,6,7-tetrahydrobenzo[b]thiophen-2-yl)-3-(4-methoxybenzyl)urea (**5i**).* Yellow solid; yield 53.1%; m.p.: 114–115.5 ℃; Rf = 0.50 (EtOAc/petroleum ether = 1/4), ^{1}H NMR (600 MHz, DMSO-d_6) δ 10.05 (s, 1H), 7.44 (t, J = 5.7 Hz 1H), 7.22 (d, J = 8.2 Hz, 2H), 6.90 (d, J = 8.2 Hz, 2H), 4.24 (d, J = 5.7 Hz, 2H), 3.72 (s, 3H), 3.15 (d, J = 5.1 Hz, 1H), 2.75 (d, J = 6.3 Hz, 1H), 2.47 (m, 1H), 1.77 (m, 2H), 1.71 (d, J = 4.4 Hz, 1H), 1.54–1.51 (m, 1H), 1.19 (d, J = 6.9 Hz, 3H). ^{13}C NMR (150 MHz, DMSO-d_6) δ 158.1, 153.3, 150.5, 134.3, 130.9, 128.3, 124.5, 114.8, 113.5, 88.0, 54.8, 42.2, 29.4, 27.9, 23.3, 20.3, 18.8. HRMS (ESI+): *m/z* calcd for $C_{19}H_{21}N_3O_2^+$ $[M + H]^+$: 356.1433, found: 356.1405.

*4.2.3.10. 1-(3-Cyano-4,7-dihydro-5H-thieno[2,3-c]pyran-2-yl)-3-(4-methoxybenzyl)urea (**5j**).* Light yellow solid; yield 62.8%; m.p.: 218–219 ℃; Rf = 0.65 (EtOAc/petroleum ether = 1/2), ^{1}H NMR (600 MHz, DMSO-d_6) δ 10.08 (s, 1H), 7.22 (d, J = 8.6 Hz, 2H), 7.17 (t, J = 5.8 Hz, 1H), 6.90 (d, J = 8.6 Hz, 2H), 4.55 (s, 2H), 4.26 (d, J = 5.8 Hz, 2H), 3.85 (t, J = 5.5 Hz, 2H), 3.73 (s, 3H), 2.54 (t, J = 5.5 Hz, 2H). ^{13}C NMR (150 MHz, DMSO-d_6) δ 158.8, 153.8, 151.7, 131.5, 129.1, 128.3, 123.3, 114.9, 114.3, 88.8, 64.2, 64.2, 55.5, 43.0, 24.4. HRMS (ESI+): *m/z* calcd for $C_{17}H_{17}N_3O_3^+$ $[M + H]^+$: 344.1069, found: 344.1060.

*4.2.3.11. 1-(3-Cyano-6-methyl-4,5,6,7-tetrahydrothieno[2,3-c]pyridin-2-yl)-3-(4-methoxybenzyl)urea (**5k**).* Brick red solid; yield 65.4%; m.p.: 201.5–203 ℃; Rf = 0.35 (acetone/petroleum ether = 1/1), ^{1}H NMR (600 MHz, $CDCl_3$) δ 8.86 (s, 1H), 7.23 (d, J = 8.6 Hz, 2H), 6.84 (d, J = 8.6 Hz, 2H), 6.14 (t, J = 5.7 Hz, 1H), 4.38 (d, J = 5.7 Hz, 2H), 3.77 (s, 3H), 3.34 (d, J = 1.9 Hz, 2H), 2.68 (t, J = 5.8 Hz, 2H), 2.59 (t, J = 5.8 Hz, 2H), 2.42 (s, 3H). ^{13}C NMR (150 MHz, $CDCl_3$) δ 159.0, 153.5, 152.2, 130.4, 129.0, 128.3, 123.2, 115.6, 114.1, 55.3, 52.6, 51.6, 45.3, 43.7, 29.7, 24.2. HRMS (ESI+): *m/z* calcd for $C_{18}H_{20}N_4O_2^+$ $[M + H]^+$: 357.1385, found: 357.1370.

*4.2.3.12. 1-(4-Methoxybenzyl)-3-(5-nitrothiazol-2-yl)urea (**5l**).* Light yellow solid; yield 47.2%; m.p.: 192–193 ℃; Rf = 0.40 (acetone/petroleum ether = 1/2), ^{1}H NMR (600 MHz, DMSO-d_6) δ 11.62 (s, 1H), 8.50 (s, 1H), 7.24 (d, J = 8.6 Hz, 3H), 6.90 (d, J = 8.6 Hz, 2H), 4.30 (d, J = 5.9 Hz, 2H), 3.73 (s, 3H). ^{13}C NMR (150 MHz, DMSO-d_6) δ 164.8, 158.9, 153.8, 143.9, 131.2, 129.2, 128.8, 114.3, 55.5, 43.1. HRMS (ESI+): *m/z* calcd for $C_{12}H_{12}N_4O_4$ $[M + H]^+$: 309.0658, found: 309.0663.

*4.2.3.13. 1-(4-Methoxybenzyl)-3-(4,5,6,7-tetrahydrobenzo[d]thiazol-2-yl)urea (**5m**).* White solid; yield 51.9%; m.p.: 171–172 ℃; Rf = 0.25 (EtOAc/petroleum ether = 1/1), ^{1}H NMR (600 MHz, $CDCl_3$) δ 7.21 (d, J = 8.6 Hz, 2H), 6.83 (d, J = 8.6 Hz, 2H), 4.40 (d, J = 5.7 Hz, 2H), 3.78 (s, 3H), 2.61 (m, 2H), 2.56 (m, 2H), 1.80 (m, 4H). ^{13}C NMR (150 MHz, $CDCl_3$) δ 159.3, 158.8, 155.0, 144.1, 130.8, 128.7, 120.2, 113.9, 55.3, 43.4, 26.6, 23.3, 22.9, 22.9. HRMS (ESI+): *m/z* calcd for $C_{16}H_{19}N_3O_2^+$ $[M + H]^+$: 318.1276, found: 318.1293.

*4.2.3.14. 1-(4-Methoxybenzyl)-3-(7-oxo-4,5,6,7-tetrahydrobenzo[d]thiazol-2-yl)urea (**5n**).* White solid; yield 78.3%; m.p.: 233–234 ℃; Rf = 0.70 (MeOH/CH_2Cl_2 = 5/95), ^{1}H NMR (600 MHz, DMSO-d_6) δ 11.00 (s, 1H), 7.22 (d, J = 8.7 Hz, 2H), 7.09 (d, J = 6.4 Hz, 1H), 6.90 (d, J = 8.7 Hz, 2H), 4.26 (d, J = 5.9 Hz, 2H), 3.72 (s, 3H), 2.78 (t, J = 6.3 Hz, 2H), 2.44 (t, J = 6.4 Hz, 2H), 2.04 (p, J = 6.3 Hz, 2H). ^{13}C NMR (150 MHz, DMSO-d_6) δ 191.5, 165.0, 164.7, 158.4, 153.2, 131.0, 128.7, 122.5, 113.8, 55.1, 42.5, 37.1, 26.4, 22.6. HRMS (ESI+): *m/z* calcd for $C_{16}H_{17}N_3O_3^+$ $[M + H]^+$: 332.1069, found: 332.1062.

*4.2.4. Synthesis of compounds **6b-6v** and **7a-7g***

Compounds **6b-6v, 7a-7g** were prepared from a series of starting materials **3** according to the General method B.

*4.2.4.1. N-(2-methoxybenzyl)-1H-imidazole-1-carboxamide (**6b**).* Rf = 0.60 (MeOH/CH_2Cl_2 = 5/95), ^{1}H NMR (600 MHz, $CDCl_3$) δ 8.06 (d, J = 1.1 Hz, 1H), 7.35–7.27 (m, 3H), 7.02 (dd, J = 1.6, 0.9 Hz, 1H), 6.94 (td, J = 7.5, 1.1 Hz, 1H), 6.90 (dd, J = 8.2, 1.0 Hz, 1H), 6.73 (d, J = 6.0 Hz, 1H), 4.57 (d, J = 5.8 Hz, 2H), 3.87 (s, 3H). ^{13}C NMR (150 MHz, $CDCl_3$) δ 157.6, 148.9, 136.0, 130.4, 130.2, 129.7, 125.0, 121.0, 116.0, 110.7, 55.6, 41.2.

*4.2.4.2. N-(3-methoxybenzyl)-1H-imidazole-1-carboxamide (**6c**).* Rf = 0.55 (MeOH/CH_2Cl_2 = 5/95), ^{1}H NMR (600 MHz, $CDCl_3$) δ 8.07 (s, 1H), 7.79 (d, J = 5.8 Hz, 1H), 7.43 (t, J = 1.5 Hz, 1H), 7.24 (t, J = 7.9 Hz, 1H), 6.90–6.80 (m, 4H), 4.51 (d, J = 5.6 Hz, 2H), 3.76 (s, 3H). ^{13}C NMR (150 MHz, $CDCl_3$) δ 160.0, 149.2, 138.8, 135.9, 130.0, 129.9, 120.2, 116.6, 113.9, 113.2, 55.4, 44.9.

*4.2.4.3. N-benzyl-1H-imidazole-1-carboxamide (**6d**).* Rf = 0.70 (MeOH/CH_2Cl_2 = 5/95), ^{1}H NMR (600 MHz, $CDCl_3$) δ 8.05 (t, J = 1.1 Hz, 1H), 7.92 (t, J = 5.8 Hz, 1H), 7.43 (t, J = 1.5 Hz, 1H), 7.36–7.24 (m, 5H), 6.85 (t, J = 1.2 Hz, 1H), 4.53 (d, J = 5.6 Hz, 2H). ^{13}C NMR (150 MHz, $CDCl_3$) δ 149.2, 137.3, 135.9, 129.7, 128.9, 128.0, 116.7.

*4.2.4.4. N-(2-methylbenzyl)-1H-imidazole-1-carboxamide (**6e**).* Rf = 0.50 (MeOH/CH_2Cl_2 = 5/95), ^{1}H NMR (600 MHz, $CDCl_3$) δ 7.95 (t, J = 1.1 Hz, 1H), 7.39 (t, J = 1.5 Hz, 1H), 7.25 (d, J = 1.7 Hz, 1H), 7.21–7.14 (m, 3H), 6.89–6.84 (m, 1H), 4.56 (d, J = 5.2 Hz, 2H), 2.34 (s, 3H). ^{13}C NMR (150 MHz, $CDCl_3$) δ 148.9, 136.7, 135.9, 134.7, 130.9, 130.0, 128.9, 128.4, 126.5, 116.5, 43.2, 19.2.

*4.2.4.5. N-(3-methylbenzyl)-1H-imidazole-1-carboxamide (**6f**).* Rf = 0.50 (MeOH/CH_2Cl_2 = 5/95), ^{1}H NMR (600 MHz, $CDCl_3$) δ 8.05 (d, J = 1.2 Hz, 1H), 7.71–7.66 (m, 1H), 7.43 (t, J = 1.4 Hz, 1H), 7.21 (t, J = 7.5 Hz, 1H), 7.14–7.07 (m, 3H), 6.90–6.87 (m, 1H), 4.51 (d, J = 5.6 Hz, 2H), 2.32 (s, 3H). ^{13}C NMR (150 MHz, $CDCl_3$) δ 149.1, 138.7, 137.2, 135.9, 129.8, 128.9, 128.8, 128.8, 125.1, 116.6, 45.0, 21.5.

*4.2.4.6. N-(4-methylbenzyl)-1H-imidazole-1-carboxamide (**6g**).* Rf = 0.50 (MeOH/CH_2Cl_2 = 5/95), ^{1}H NMR (600 MHz, $CDCl_3$) δ 8.07 (t, J = 1.1 Hz, 1H), 7.48 (d, J = 5.3 Hz, 1H), 7.40 (t, J = 1.5 Hz, 1H), 7.20 (d, J = 8.1 Hz, 2H), 7.14 (d, J = 7.8 Hz, 2H), 6.90 (t, J = 1.2 Hz, 1H), 4.51 (d, J = 5.6 Hz, 2H), 2.33 (s, 3H). ^{13}C NMR (150 MHz, $CDCl_3$) δ 149.1, 137.9, 135.9, 134.2, 130.0, 129.6, 128.1, 116.5, 44.8, 21.2.

*4.2.4.7. N-(4-fluorobenzyl)-1H-imidazole-1-carboxamide (**6h**).* Rf = 0.50 (MeOH/CH_2Cl_2 = 5/95), ^{1}H NMR (600 MHz, $CDCl_3$) δ 8.10 (t, J = 1.1 Hz, 1H), 7.90 (t, J = 5.6 Hz, 1H), 7.43 (t, J = 1.5 Hz, 1H), 7.28 (dd, J = 8.5, 5.4 Hz, 2H), 7.01 (t, J = 8.6 Hz, 2H), 6.87 (t, J = 1.2 Hz, 1H), 4.51 (d, J = 5.7 Hz, 2H). ^{13}C NMR (150 MHz, $CDCl_3$) δ 149.0, 135.8, 129.7, 129.7, 129.6, 116.6, 115.8, 115.6, 44.2.

*4.2.4.8. 1,3-bis(2-chlorobenzyl)urea (**6i**).* Rf = 0.45 (MeOH/CH_2Cl_2 = 5/95), ^{1}H NMR (600 MHz, DMSO-d_6) δ 7.42 (dd, J = 7.8, 1.3 Hz, 2H), 7.37–7.31 (m, 4H), 7.28 (td, J = 7.5, 2.0 Hz, 2H), 6.62 (t, J = 6.1 Hz, 2H), 4.30 (d, J = 6.1 Hz, 4H). ^{13}C NMR (150 MHz, DMSO-d_6) δ 157.8, 137.8, 131.9, 129.0, 128.6, 128.4, 127.1, 40.9.

*4.2.4.9. N-(3-chlorobenzyl)-1H-imidazole-1-carboxamide (**6j**).* Rf = 0.45 (MeOH/CH_2Cl_2 = 5/95), ^{1}H NMR (600 MHz, $CDCl_3$) δ 8.33 (t, J = 5.8 Hz, 1H), 8.19 (t, J = 1.2 Hz, 1H), 7.49 (t, J = 1.5 Hz, 1H), 7.28 (dt, J = 2.6, 1.2 Hz, 1H), 7.24 (dd, J = 4.8, 1.1 Hz, 2H), 7.19 (ddd, J = 5.0, 4.1, 1.7 Hz, 1H), 6.89 (t, J = 1.2 Hz, 1H), 4.50 (d, J = 5.8 Hz, 2H). ^{13}C NMR (150 MHz, $CDCl_3$) δ 149.2, 139.5, 136.0, 134.7, 130.2, 129.5, 128.1, 128.0, 126.1, 116.9, 44.3.

*4.2.4.10. N-(4-chlorobenzyl)-1H-imidazole-1-carboxamide (**6k**).* Rf = 0.45 (MeOH/CH_2Cl_2 = 5/95), ^{1}H NMR (600 MHz, DMSO-d_6) δ 9.10 (t, J = 5.9 Hz, 1H), 8.27 (t, J = 1.2 Hz, 1H), 7.70 (t, J = 1.5 Hz, 1H), 7.43–7.39 (m, 2H), 7.37 (d, J = 8.5 Hz, 2H), 7.06–7.02 (m, 1H), 4.45 (d, J = 5.8 Hz, 2H). ^{13}C NMR (150 MHz, DMSO-d_6) δ 149.0, 137.5, 136.0, 131.7, 129.7, 129.2, 128.8, 128.4, 128.1, 116.6, 42.9.

*4.2.4.11. 1,3-bis(2-bromobenzyl)urea (**6l**).* Rf = 0.45 (MeOH/CH_2Cl_2 = 5/95), ^{1}H NMR (600 MHz, DMSO-d_6) δ 7.59 (d, J = 7.9 Hz, 2H), 7.35 (dd, J = 18.1, 7.4 Hz, 4H), 7.25–7.15 (m, 2H), 6.66 (t, J = 6.1 Hz, 2H), 4.26 (d, J = 6.0 Hz, 4H). ^{13}C NMR (150 MHz, DMSO-d_6) δ 157.8, 139.3, 132.3, 128.7, 128.7, 127.7, 122.3, 43.4.

*4.2.4.12. N-(3-bromobenzyl)-1H-imidazole-1-carboxamide (**6m**).* Rf = 0.45 (MeOH/CH_2Cl_2 = 5/95), ^{1}H NMR (600 MHz, DMSO-d_6) δ 9.10 (t, J = 5.9 Hz, 1H), 8.28 (t, J = 1.1 Hz, 1H), 7.71 (t, J = 1.5 Hz, 1H), 7.56 (d, J = 1.8 Hz, 1H), 7.50–7.47 (m, 1H), 7.37 (dt, J = 7.8, 1.4 Hz, 1H), 7.33 (d, J = 7.8 Hz, 1H), 7.05 (t, J = 1.2 Hz, 1H), 4.47 (d, J = 5.8 Hz, 2H). ^{13}C NMR (150 MHz, DMSO-d_6) δ 149.0, 141.3, 136.0, 130.7, 130.1, 130.0, 129.7, 126.4, 121.7, 116.6, 43.0.

*4.2.4.13. N-(4-bromobenzyl)-1H-imidazole-1-carboxamide (**6n**).* Rf = 0.45 (MeOH/CH_2Cl_2 = 5/95), ^{1}H NMR (600 MHz, DMSO-d_6) δ 9.10 (t, J = 5.8 Hz, 1H), 8.27 (d, J = 1.3 Hz, 1H), 7.70 (t, J = 1.4 Hz, 1H), 7.57–7.53 (m, 2H), 7.34–7.29 (m, 2H), 7.04 (t, J = 1.2 Hz, 1H), 4.43 (d, J = 5.8 Hz, 2H). ^{13}C NMR (150 MHz, DMSO-d_6) δ 149.0, 138.0, 136.0, 131.3, 129.7, 129.6, 120.2 , 116.6, 42.9.

*4.2.4.14. N-(4-ethoxybenzyl)-1H-imidazole-1-carboxamide (**6o**).* Rf = 0.60 (MeOH/CH_2Cl_2 = 5/95), ^{1}H NMR (600 MHz, DMSO-d_6) δ 8.07 (s, 1H), 7.63–7.55 (m, 1H), 7.41 (s, 1H), 7.21 (d, J = 8.6 Hz, 2H), 6.89 (s, 1H), 6.84 (d, J = 8.6 Hz, 2H), 4.46 (d, J = 5.5 Hz, 2H), 4.02–3.98 (m, 2H), 1.40 (d, J = 7.0 Hz, 3H). ^{13}C NMR (150 MHz, DMSO-d_6) δ 158.8, 149.1, 135.9, 129.9, 129.5, 129.2, 116.5, 114.8, 63.6, 44.5, 15.0.

*4.2.4.15. N-(2-ethoxybenzyl)-1H-imidazole-1-carboxamide (**6p**).* Rf = 0.60 (MeOH/CH_2Cl_2 = 5/95), ^{1}H NMR (600 MHz, DMSO-d_6) δ 9.08–8.96 (m, 1H), 8.34 (d, J = 1.4 Hz, 1H), 7.79 (q, J = 1.5 Hz, 1H), 7.24 (dd, J = 8.0, 6.4 Hz, 2H), 7.04 (t, J = 1.1 Hz, 1H), 6.98 (d, J = 8.3 Hz, 1H), 6.91 (t, J = 7.3 Hz, 1H), 4.45 (d, J = 5.7 Hz, 2H), 4.06 (q, J = 6.9 Hz, 2H), 1.33 (t, J = 7.0 Hz, 3H). ^{13}C NMR (150 MHz, DMSO-d_6) δ 156.0, 148.9, 136.1, 129.5, 128.4, 127.7, 125.9, 120.1, 116.7, 111.5, 63.3, 38.8, 14.7.

*4.2.4.16. N-(3,4-dimethoxybenzyl)-1H-imidazole-1-carboxamide (**6q**).* Rf = 0.50 (MeOH/CH_2Cl_2 = 5/95), ^{1}H NMR (600 MHz, $CDCl_3$) δ 8.12 (s, 1H), 7.73–7.67 (m, 1H), 7.46 (s, 1H), 6.92–6.88 (m, 1H), 6.84 (dd, J = 8.1, 2.0 Hz, 1H), 6.80 (d, J = 2.0 Hz, 1H), 6.77 (d, J = 8.1 Hz, 1H), 4.46 (d, J = 5.5 Hz, 2H), 3.81 (s, 3H), 3.78 (s, 3H). ^{13}C NMR (150 MHz, $CDCl_3$) δ 149.1, 149.1, 148.7, 136.0, 129.8, 129.8, 120.6, 116.6, 111.5, 111.3, 56.0, 55.9, 44.9.

*4.2.4.17. N-(2,4-dimethoxybenzyl)-1H-imidazole-1-carboxamide (**6r**).* Rf = 0.50 (MeOH/CH_2Cl_2 = 5/95), ^{1}H NMR (600 MHz, $CDCl_3$) δ 8.06 (t, J = 1.1 Hz, 1H), 7.35 (t, J = 1.5 Hz, 1H), 7.21 (d, J = 8.1 Hz, 1H), 6.99–6.96 (m, 1H), 6.95 (d, J = 5.9 Hz, 1H), 6.46–6.42 (m, 2H), 4.48 (d, J = 5.6 Hz, 2H), 3.81 (s, 3H), 3.78 (s, 3H). ^{13}C NMR (150 MHz, $CDCl_3$) δ 161.0, 158.6, 148.9, 136.0, 130.9, 130.2, 117.6, 116.1, 104.2, 98.8, 55.6, 55.5, 40.6.

*4.2.4.18. N-(3,5-dimethoxybenzyl)-1H-imidazole-1-carboxamide (**6s**).* Rf = 0.50 (MeOH/CH_2Cl_2 = 5/95), ^{1}H NMR (600 MHz, $CDCl_3$) δ 8.10 (t, J = 1.2 Hz, 1H), 7.90 (s, 1H), 7.44 (d, J = 1.6 Hz, 1H), 6.91–6.88 (m, 1H), 6.44 (d, J = 2.3 Hz, 2H), 6.35 (t, J = 2.3 Hz, 1H), 4.46 (d, J = 5.7 Hz, 2H), 3.74 (s, 6H). ^{13}C NMR (150 MHz, $CDCl_3$) δ 161.2, 149.2, 139.6, 135.9, 129.8, 116.7, 106.0, 99.6, 55.5, 45.0.

*4.2.4.19. N-benzyl-N-methyl-1H-imidazole-1-carboxamide (**7a**).* Rf = 0.75 (MeOH/CH_2Cl_2 = 5/95),^{1}H NMR (600 MHz, DMSO-d_6) δ 7.92 (t, J = 1.1 Hz, 1H), 7.39 (dd, J = 8.1, 6.7 Hz, 2H), 7.35–7.32 (m, 1H), 7.28 (d, J = 7.5 Hz, 2H), 7.24 (t, J = 1.5 Hz, 1H), 7.06 (t, J = 1.2 Hz, 1H), 4.63 (s, 2H), 3.03 (s, 3H). ^{13}C NMR (150 MHz, DMSO-d_6) δ 152.2, 137.1, 135.4, 129.8, 129.2, 128.3, 127.6, 118.1, 54.2, 36.5.

*4.2.5. Synthesis of compounds **8b-8v**, and **9a-9g***

Compounds **8b-8v** and **9a-9g** are correspondingly prepared from intermediates **6b-6v** and **7a-7g**, respectively, according to the General method C.

*4.2.5.1. 1-(3-cyano-4,5,6,7-tetrahydrobenzo[b]thiophen-2-yl)-3-(2-methoxybenzyl)urea (**8b**).* White solid; yield 77.5%; m.p.: 200–201 ℃; Rf = 0.25 (EtOAc/petroleum ether = 1/6), ^{1}H NMR (600 MHz, $CDCl_3$) δ 8.59 (s, 1H), 7.29 (dd, J = 7.6, 1.7 Hz, 1H), 7.24 (dd, J = 7.6, 1.7 Hz, 1H), 6.89 (t, J = 7.4 Hz, 1H), 6.85 (d, J = 8.2 Hz, 1H), 6.11 (t, J = 6.0 Hz, 1H), 4.45 (d, J = 6.0 Hz, 2H), 3.84 (s, 3H), 2.55 (m, 2H), 2.46 (m, 2H), 1.81–1.77 (m, 4H). ^{13}C NMR (150 MHz, $CDCl_3$) δ 157.6, 153.7, 151.9, 130.0, 129.5, 128.9, 126.6, 126.2, 120.7, 116.1, 110.3, 55.5, 40.3, 29.8, 24.1, 24.0, 23.3, 22.3. HRMS (ESI+): *m/z* calcd for $C_{18}H_{19}N_3O_2^+$ [M + H]$^+$: 342.1276, found: 342.1283.

*4.2.5.2. 1-(3-Cyano-4,5,6,7-tetrahydrobenzo[b]thiophen-2-yl)-3-(3-methoxybenzyl)urea (**8c**).* White solid; yield 75.8%; m.p.: 147–148 ℃; Rf = 0.25 (EtOAc/petroleum ether = 1/6), ^{1}H NMR (600 MHz, $CDCl_3$) δ 8.74 (s, 1H), 7.22 (t, J = 7.9 Hz, 1H), 6.88 (d, J = 7.9 Hz, 1H), 6.85 (t, J = 2.0 Hz 1H), 6.78 (dd, J = 8.1, 2.5 Hz, 1H), 6.09 (t, J = 5.7 Hz, 1H), 4.43 (d, J = 5.7 Hz, 2H), 3.77 (s, 3H), 2.55 (t, J = 5.8 Hz, 2H), 2.41 (t, J = 5.8 Hz, 2H), 1.81–1.76 (m, 4H). ^{13}C NMR (150 MHz, $CDCl_3$) δ 160.0, 153.8, 151.8, 139.9, 130.2, 129.8, 126.3, 119.8, 116.2, 113.1, 112.9, 89.2, 55.3, 44.3, 24.0, 24.0, 23.3, 22.3. HRMS (ESI+): *m/z* calcd for $C_{18}H_{19}N_3O_2^+$ [M + H]$^+$: 342.1276, found: 342.1243.

*4.2.5.3. 1-Benzyl-3-(3-cyano-4,5,6,7-tetrahydrobenzo[b]thiophen-2-yl) urea (**8d**).* White solid; yield 64.1%; m.p.: 209.5–210.5 ℃; Rf = 0.35 (EtOAc/petroleum ether = 1/6), ^{1}H NMR (600 MHz, $CDCl_3$) δ 8.68 (s, 1H), 7.33–7.25 (m, 5H), 6.02 (t, J = 5.7 Hz, 1H), 4.47 (d, J = 5.7 Hz, 2H), 2.56 (t, J = 5.9 Hz, 2H), 2.41 (t, J = 5.9 Hz, 2H), 1.81–1.76 (m, 4H). ^{13}C NMR (150 MHz, $CDCl_3$) δ 153.7, 151.8, 138.4, 130.2, 128.8, 127.6, 127.6, 126.3, 116.3, 60.6, 44.4, 24.0, 24.0, 23.3, 22.3. HRMS (ESI+): *m/z* calcd for $C_{17}H_{17}N_3O^+$ [M + H]$^+$: 312.1171, found: 312.1214.

*4.2.5.4. 1-(3-Cyano-4,5,6,7-tetrahydrobenzo[b]thiophen-2-yl)-3-(2-methylbenzyl)urea (**8e**).* White solid; yield 78.7%; m.p.: 205.5–206 ℃; Rf = 0.35 (EtOAc/petroleum ether = 1/4), ^{1}H NMR (600 MHz, $CDCl_3$) δ 8.64 (s, 1H), 7.28 (d, J = 6.8 Hz, 1H), 7.17 (m, 3H), 5.90 (t, J = 5.5 Hz, 1H), 4.45 (d, J = 5.5 Hz, 2H), 2.57 (t, J = 5.5 Hz, 2H), 2.37 (t, J = 6.0 Hz, 2H), 2.35 (s, 3H), 1.84–1.76 (m, 4H). ^{13}C NMR (150 MHz, $CDCl_3$) δ 153.5, 152.1, 136.3, 136.1, 130.6, 130.1, 128.2, 127.8, 126.3, 126.3, 116.4, 88.8, 42.5, 24.0, 23.3, 22.3, 19.2. HRMS (ESI+): *m/z* calcd for $C_{18}H_{19}N_3O^+$ $[M + H]^+$: 326.1327, found: 326.1372.

*4.2.5.5. 1-(3-Cyano-4,5,6,7-tetrahydrobenzo[b]thiophen-2-yl)-3-(3-methylbenzyl)urea (**8f**).* White solid; yield 81.4%; m.p.: 181–182 ℃; Rf = 0.35 (EtOAc/petroleum ether = 1/4), ^{1}H NMR (600 MHz, $CDCl_3$) δ 8.70 (s, 1H), 7.20 (t, J = 7.5 Hz, 1H), 7.13–7.08 (m, 2H), 7.07 (d, J = 7.5 Hz, 1H), 6.03 (t, J = 5.7 Hz, 1H), 4.42 (d, J = 5.7 Hz, 2H), 2.56 (t, J = 5.9 Hz, 2H), 2.40 (t, J = 5.9 Hz, 2H), 2.32 (s, 3H), 1.83–1.76 (m, 4H). ^{13}C NMR (150 MHz, $CDCl_3$) δ 153.8, 151.8, 138.5, 138.3, 130.2, 128.7, 128.3, 128.3, 126.3, 124.6, 116.3, 89.1, 44.4, 24.0, 24.0, 23.3, 22.3, 21.5. HRMS (ESI+): *m/z* calcd for $C_{18}H_{19}N_3O^+$ $[M + H]^+$: 326.1327, found: 326.1355.

*4.2.5.6. 1-(3-Cyano-4,5,6,7-tetrahydrobenzo[b]thiophen-2-yl)-3-(4-methylbenzyl)urea (**8g**).* White solid; yield 80.7%; m.p.: 194–195.5 ℃; Rf = 0.35 (EtOAc/petroleum ether = 1/4), ^{1}H NMR (600 MHz, $CDCl_3$) δ 8.68 (s, 1H), 7.19 (d, J = 7.8 Hz, 2H), 7.11 (d, J = 7.8 Hz, 2H), 6.03 (t, J = 5.6 Hz, 1H), 4.40 (d, J = 5.6 Hz, 2H), 2.56 (t, J = 5.9 Hz, 2H), 2.40 (t, J = 5.9 Hz, 2H), 2.32 (s, 3H), 1.84–1.74 (m, 4H). ^{13}C NMR (150 MHz, $CDCl_3$) δ 153.7, 151.9, 137.2, 135.3, 130.1, 129.4, 127.6, 126.2, 116.2, 89.1, 44.2, 24.0, 24.0, 23.3, 22.3, 21.2. HRMS (ESI+): *m/z* calcd for $C_{18}H_{19}N_3O^+$ $[M + H]^+$: 326.1327, found: 326.1331.

*4.2.5.7. 1-(3-Cyano-4,5,6,7-tetrahydrobenzo[b]thiophen-2-yl)-3-(4-fluorobenzyl)urea (**8h**).* Light yellow solid; yield 47.2%; m.p.: 218–219 ℃; Rf = 0.30 (EtOAc/petroleum ether = 1/6), ^{1}H NMR (600 MHz, $CDCl_3$) δ 8.67 (s, 1H), 7.27 (dd, J = 8.6, 5.4 Hz, 2H), 7.00 (t, J = 8.6 Hz, 2H), 6.04 (t, J = 5.7 Hz, 1H), 4.42 (d, J = 5.7 Hz, 2H), 2.59–2.53 (m, 2H), 2.40 (t, J = 5.6 Hz, 2H), 1.79 (m, 4H). ^{13}C NMR (150 MHz, $CDCl_3$) δ 162.3 (d, J = 245.7 Hz), 153.7, 151.7, 134.2, 134.2, 130.2, 129.4, 129.3, 126.5, 116.3, 115.7, 115.5, 89.2, 43.7, 24.0, 24.0, 23.3, 22.2. HRMS (ESI+): *m/z* calcd for $C_{17}H_{16}FN_3^+$ $[M + H]^+$: 330.1076, found: 330.1086.

*4.2.5.8. 1-(2-Chlorobenzyl)-3-(3-cyano-4,5,6,7-tetrahydrobenzo[b]thiophen-2-yl)urea (**8i**).* White solid; yield 80.7%; m.p.: 200.5–202 ℃; Rf = 0.30 (EtOAc/petroleum ether = 1/6), ^{1}H NMR (600 MHz, $CDCl_3$) δ 10.08 (s, 1H), 7.46 (dd, J = 7.5, 1.8 Hz, 1H), 7.39 (dd, J = 7.5, 1.8 Hz, 1H), 7.36–7.31 (m, 2H), 7.29 (t, J = 5.9 Hz, 1H), 4.40 (d, J = 5.9 Hz, 2H), 2.54–2.50 (m, 2H), 2.47–2.40 (m, 2H), 1.77–1.67 (m, 4H). ^{13}C NMR (150 MHz, $CDCl_3$) δ 153.4, 150.1, 136.4, 132.2, 129.9, 129.4, 129.1, 127.5, 127.3, 125.0, 114.9, 88.9, 41.2, 23.5, 23.3, 22.7, 21.8. HRMS (ESI+): *m/z* calcd for $C_{17}H_{16}ClN_3^+$ $[M + H]^+$: 346.0781, found: 346.0799, 348.0756.

*4.2.5.9. 1-(3-Chlorobenzyl)-3-(3-cyano-4,5,6,7-tetrahydrobenzo[b]thiophen-2-yl)urea (**8J**).* White solid; yield 71.1%; m.p.: 216.5–218 ℃; Rf = 0.30 (EtOAc/petroleum ether = 1/6), ^{1}H NMR (600 MHz, DMSO-d_6) δ 10.04 (s, 1H), 7.40–7.24 (m, 5H), 4.34 (d, J = 6.0 Hz, 2H), 2.52 (d, J = 4.8 Hz, 2H), 2.44 (d, J = 6.0 Hz, 2H), 1.74–1.70 (m, 4H). ^{13}C NMR (150 MHz, DMSO-d_6) δ 153.5, 150.1, 142.1, 133.1, 130.3, 129.8, 126.9, 125.8, 125.0, 114.8, 89.0, 42.5, 23.5, 23.3, 22.7, 21.8. HRMS (ESI+): *m/z* calcd for $C_{17}H_{16}ClN_3^+$ $[M + H]^+$: 346.0781, found: 346.0799, 348.0672

*4.2.5.10. 1-(4-Chlorobenzyl)-3-(3-cyano-4,5,6,7-tetrahydrobenzo[b]thiophen-2-yl)urea (**8k**).* White solid; yield 67.1%; m.p.: 210.5–211 ℃; Rf = 0.30 (EtOAc/petroleum ether = 1/6), ^{1}H NMR (600 MHz, DMSO-d_6) δ 10.03 (s, 1H), 7.40 (d, J = 8.1 Hz, 2H), 7.31 (d, J = 8.1 Hz, 2H), 7.25 (t, J = 5.9 Hz, 1H), 4.32 (d, J = 5.9 Hz, 2H), 2.52 (t, J = 5.2 Hz, 2H), 2.43 (d, J = 5.2 Hz, 2H), 1.77–1.67 (m, 4H). ^{13}C NMR (150 MHz, DMSO-d_6) δ 153.5, 150.2, 138.5, 131.5, 129.8, 129.0, 128.4, 124.9, 114.8, 88.9, 42.4, 23.5, 23.3, 22.7, 21.8. HRMS (ESI+): *m/z* calcd for $C_{17}H_{16}ClN_3^+$ $[M + H]^+$: 346.0781, found: 346.0790, 348.0756.

*4.2.5.11. 1-(2-Bromobenzyl)-3-(3-cyano-4,5,6,7-tetrahydrobenzo[b]thiophen-2-yl)urea (**8l**).* White solid; yield 68.9%; m.p.: 201–202 ℃; Rf = 0.40 (EtOAc/petroleum ether = 1/4), ^{1}H NMR (600 MHz, DMSO-d_6) δ 10.11 (s, 1H), 7.63 (dd, J = 7.9, 1.1 Hz, 1H), 7.41–7.36 (m, 2H), 7.30 (t, J = 6.0 Hz, 1H), 7.24 (ddd, J = 7.9, 6.5, 2.6 Hz, 1H), 4.37 (d, J = 6.0 Hz, 2H), 2.54–2.51 (m, 2H), 2.46–2.42 (m, 2H), 1.78–1.66 (m, 4H). ^{13}C NMR (150 MHz, DMSO-d_6) δ 153.4, 150.1, 137.9, 132.5, 129.8, 129.3, 129.2, 127.9, 125.0, 122.5, 114.8, 88.9, 43.6, 23.5, 23.3, 22.7, 21.8. HRMS (ESI+): *m/z* calcd for $C_{17}H_{16}BrN_3^+$ $[M + H]^+$: 390.0276, found: 390.0288, 392.0271.

*4.2.5.12. 1-(3-Bromobenzyl)-3-(3-cyano-4,5,6,7-tetrahydrobenzo[b]thiophen-2-yl)urea (**8m**).* White solid; yield 70.5%; m.p.: 213–214 ℃; Rf = 0.40 (EtOAc/petroleum ether = 1/4), ^{1}H NMR (600 MHz, DMSO-d_6) δ 10.05 (s, 1H), 7.49 (s, 1H), 7.45 (dt, J = 6.3, 2.5 Hz, 1H), 7.31 (d, J = 4.1 Hz, 2H), 7.26 (t, J = 6.0 Hz, 1H), 4.33 (d, J = 6.0 Hz, 2H), 2.52 (t, J = 3.2 Hz, 2H), 2.43 (t, J = 3.2 Hz, 2H), 1.72 (m, 4H). ^{13}C NMR (150 MHz, DMSO-d_6) δ 153.5, 150.1, 142.3, 130.6, 129.8, 129.8, 126.2, 125.0, 121.7, 114.8, 89.0, 42.5, 23.5, 23.3, 22.7, 21.8. HRMS (ESI+): *m/z* calcd for $C_{17}H_{16}BrN_3^+$ $[M + H]^+$: 390.0276, found: 390.0256, 392.0240.

*4.2.5.13. 1-(4-Bromobenzyl)-3-(3-cyano-4,5,6,7-tetrahydrobenzo[b]thiophen-2-yl)urea (**8n**).* White solid; yield 72.6%; m.p.: 224–225.5 ℃; Rf = 0.40 (EtOAc/petroleum ether = 1/4), ^{1}H NMR (600 MHz, DMSO-d_6) δ 10.03 (s, 1H), 7.53 (d, J = 8.4 Hz, 2H), 7.25 (d, J = 8.4 Hz, 3H), 4.30 (d, J = 5.9 Hz, 2H), 2.55–2.51 (m, 2H), 2.44 (t, J = 5.1 Hz, 2H), 1.76–1.69 (m, 4H). ^{13}C NMR (150 MHz, DMSO-d_6) δ 153.5, 150.2, 138.9, 131.3, 129.8, 129.4, 124.9, 120.0, 114.8, 88.9, 42.4, 23.5, 23.3, 22.7, 21.8. HRMS (ESI+): *m/z* calcd for $C_{17}H_{16}BrN_3^+$ $[M + H]^+$: 390.0276, found: 390.0273, 392.0256.

*4.2.5.14. 1-(3-Cyano-4,5,6,7-tetrahydrobenzo[b]thiophen-2-yl)-3-(4-ethoxybenzyl)urea (**8o**).* Light yellow solid; yield 75.2%; m.p.: 186–187 ℃; Rf = 0.30 (EtOAc/petroleum ether = 1/5), ^{1}H NMR (600 MHz, $CDCl_3$) δ 8.70 (s, 1H), 7.20 (d, J = 8.6 Hz, 2H), 6.82 (d, J = 8.6 Hz, 2H), 6.04 (t, J = 5.5 Hz, 1H), 4.36 (d, J = 5.5 Hz, 2H), 3.99 (q, J = 7.0 Hz, 2H), 2.55 (t, J = 5.9 Hz, 2H), 2.39 (t, J = 5.9 Hz, 2H), 1.82–1.74 (m, 4H), 1.39 (t, J = 7.0 Hz, 3H).^{13}C NMR (150 MHz, $CDCl_3$) δ 158.4, 153.7, 151.7, 130.2, 130.2, 129.0, 126.2, 116.2, 114.7, 89.2, 63.5, 43.9, 24.0, 24.0, 23.3, 22.3, 15.0. HRMS (ESI+): *m/z* calcd for $C_{19}H_{21}N_3O_2^+$ $[M + H]^+$: 356.1433, found: 356.1456.

*4.2.5.15. 1-(3-Cyano-4,5,6,7-tetrahydrobenzo[b]thiophen-2-yl)-3-(2-ethoxybenzyl)urea (**8p**).* Light yellow solid; yield 45.6%; m.p.: 181.5–182.5 ℃; Rf = 0.30 (EtOAc/petroleum ether = 1/5), ^{1}H NMR (600 MHz, $CDCl_3$) δ 8.73 (s, 1H), 7.30 (dd, J = 7.5, 1.7 Hz, 1H), 7.21 (td, J = 7.9, 1.7 Hz, 1H), 6.87 (td, J = 7.5, 1.0 Hz, 1H), 6.82 (d, J = 7.9 Hz, 1H), 6.09 (t, J = 5.9 Hz, 1H), 4.46 (d, J = 5.9 Hz, 2H), 4.05 (q, J = 7.0 Hz, 2H), 2.54 (t, J = 6.0 Hz, 2H), 2.46–2.40 (m, 2H), 1.80–1.74 (m, 4H), 1.42 (t, J = 7.0 Hz, 3H). ^{13}C NMR (150 MHz, $CDCl_3$) δ 156.9, 153.8, 151.9, 130.0, 129.4, 128.8, 126.7, 126.1, 120.5, 116.2, 111.1, 89.0, 63.6, 40.2, 24.1, 23.9, 23.3, 22.3, 15.1. HRMS (ESI+): *m/z* calcd for $C_{19}H_{21}N_3O_2^+$ $[M + H]^+$: 356.1433, found: 356.1473.

*4.2.5.16. 1-(3-Cyano-4,5,6,7-tetrahydrobenzo[b]thiophen-2-yl)-3-(3,4-dimethoxybenzyl)urea (**8q**).* Light yellow solid; yield 71.3%; m.p.: 160–161 ℃; Rf = 0.45 (EtOAc/petroleum ether = 1/1), ^{1}H NMR (600 MHz, $CDCl_3$) δ 8.68 (s, 1H), 6.84 (d, J = 7.4 Hz, 2H), 6.78 (d, J = 8.0 Hz,

1H), 6.05 (t, $J = 5.6$ Hz, 1H), 4.38 (d, $J = 5.6$ Hz, 2H), 3.84 (s, 6H), 2.55 (t, $J = 5.9$ Hz, 2H), 2.42–2.37 (m, 2H), 1.80–1.73 (m, 4H).^{13}C NMR (150 MHz, $CDCl_3$) δ 153.7, 151.6, 149.2, 148.5, 130.9, 130.2, 126.3, 119.9, 116.1, 111.2, 111.0, 89.3, 56.0, 56.0, 44.3, 24.0, 24.0, 23.3, 22.3. HRMS (ESI+): *m/z* calcd for $C_{19}H_{21}N_3O_3^+$ $[M + H]^+$: 372.1382, found: 372.1418.

4.2.5.17. 1-(3-Cyano-4,5,6,7-tetrahydrobenzo[b]thiophen-2-yl)-3-(2,4-dimethoxybenzyl)urea ***(8r)***. Light yellow solid; yield 68.4%; m.p.: 186–187.5 ℃; Rf = 0.45 (EtOAc/petroleum ether = 1/1), ^{1}H NMR (600 MHz, $CDCl_3$) δ 8.65 (s, 1H), 7.18 (d, $J = 8.2$ Hz, 1H), 6.41 (d, $J = 2.4$ Hz, 1H), 6.38 (dd, $J = 8.2$, 2.4 Hz, 1H), 6.15 (t, $J = 5.9$ Hz, 1H), 4.37 (d, $J = 5.9$ Hz, 2H), 3.79 (s, 3H), 3.77 (s, 3H), 2.53 (t, $J = 5.7$ Hz, 2H), 2.45 (d, $J = 5.7$ Hz, 2H), 1.82–1.75 (m, 4H). ^{13}C NMR (150 MHz, $CDCl_3$) δ 160.6, 158.6, 153.7, 130.3, 130.0, 126.0, 119.1, 116.0, 103.9, 98.6, 55.5, 55.5, 39.9, 24.1, 23.9, 23.3, 22.3. HRMS (ESI+): *m/z* calcd for $C_{19}H_{21}N_3O_3^+$ $[M + H]^+$: 372.1382, found: 372.1408.

4.2.5.18. 1-(3-Cyano-4,5,6,7-tetrahydrobenzo[b]thiophen-2-yl)-3-(3,5-dimethoxybenzyl)urea ***(8s)***. ellow solid; yield 71.1%; m.p.: 193–194 ℃; Rf = 0.45 (EtOAc/petroleum ether = 1/1), ^{1}H NMR (600 MHz, $CDCl_3$) δ 8.74 (s, 1H), 6.45 (d, $J = 2.2$ Hz, 2H), 6.33 (t, $J = 2.2$ Hz, 1H), 6.10 (t, $J = 5.7$ Hz, 1H), 4.39 (d, $J = 5.7$ Hz, 2H), 3.75 (s, 6H), 2.55 (t, $J = 6.1$ Hz, 2H), 2.42 (t, $J = 6.1$ Hz, 2H), 1.83–1.73 (m, 4H).^{13}C NMR (150 MHz, $CDCl_3$) δ 161.1, 153.8, 151.7, 140.7, 130.3, 126.3, 116.2, 105.4, 99.3, 89.3, 55.4, 44.4, 24.0, 23.3, 22.3. HRMS (ESI+): *m/z* calcd for $C_{19}H_{21}N_3O_3^+$ $[M + H]^+$: 372.1382, found: 372.1388.

4.2.5.19. 1-(3-Cyano-4,5,6,7-tetrahydrobenzo[b]thiophen-2-yl)-3-(naphthalen-2-ylmethyl)urea ***(8t)***. Yellow solid; yield 65.3%; m.p.: 209–210 ℃; Rf = 0.30 (EtOAc/petroleum ether = 1/6), ^{1}H NMR (600 MHz, DMSO-d_6) δ 10.05 (s, 1H), 7.92–7.87 (m, 3H), 7.79 (s, 1H), 7.53–7.44 (m, 3H), 7.35 (t, $J = 5.9$ Hz, 1H), 4.51 (d, $J = 5.8$ Hz, 2H), 2.52 (t, $J = 5.4$ Hz, 2H), 2.44 (t, $J = 5.4$ Hz, 2H), 1.76–1.68 (m, 4H).^{13}C NMR (150 MHz, DMSO-d_6) δ 153.6, 150.3, 136.9, 132.9, 132.2, 129.8, 128.1, 127.6, 126.3, 125.8, 125.2, 124.9, 114.9, 88.8, 43.2, 23.5, 23.3, 22.7, 21.8. HRMS (ESI+): *m/z* calcd for $C_{21}H_{19}N_3O^+$ $[M + H]^+$: 362.1327, found: 362.1364.

4.2.5.20. 1-(3-Cyano-4,5,6,7-tetrahydrobenzo[b]thiophen-2-yl)-3-(naphthalen-1-ylmethyl)urea ***(8u)***. Yellow solid; yield 53.4%; m.p.: 190–191 ℃; Rf = 0.30 (EtOAc/petroleum ether = 1/6), ^{1}H NMR (600 MHz, $CDCl_3$) δ 8.65 (s, 1H), 8.00–7.97 (m, 1H), 7.82 (dd, $J = 7.9$, 1.6 Hz, 1H), 7.76 (d, $J = 8.2$ Hz, 1H), 7.50 (dd, $J = 6.7$, 1.5 Hz, 1H), 7.47–7.42 (m, 2H), 7.38 (dd, $J = 8.2$, 7.0 Hz, 1H), 6.11 (t, $J = 5.4$ Hz, 1H), 4.86 (d, $J = 5.4$ Hz, 2H), 2.52 (t, $J = 5.8$ Hz, 2H), 2.17 (t, $J = 5.8$ Hz, 2H), 1.80–1.76 (m, 2H), 1.74–1.71 (m, 2H).^{13}C NMR (150 MHz, $CDCl_3$) δ 153.5, 151.6, 133.9, 133.5, 131.4, 130.1, 128.8, 128.6, 126.7, 126.4, 126.0, 125.5, 125.5, 123.4, 116.0, 89.1, 42.4, 23.9, 23.8, 23.3, 22.3. HRMS (ESI+): *m/z* calcd for $C_{21}H_{19}N_3O^+$ $[M + H]^+$: 362.1327, found: 362.1363.

4.2.5.21. 1-([1,1′-Biphenyl]-4-ylmethyl)-3-(3-cyano-4,5,6,7-tetrahydrobenzo[b]thiophen-2-yl)urea ***(8v)***. Yellow solid; yield 48.9%; m.p.: 211–211.5 ℃; Rf = 0.45 (EtOAc/petroleum ether = 1/6), ^{1}H NMR (600 MHz, $CDCl_3$) δ 8.65 (s, 1H), 7.57–7.53 (m, 4H), 7.42 (t, $J = 7.7$ Hz, 2H), 7.38 (d, $J = 8.1$ Hz, 2H), 7.36–7.32 (m, 1H), 6.07 (t, $J = 5.6$ Hz, 1H), 4.51 (d, $J = 5.6$ Hz, 2H), 2.54 (t, $J = 5.6$ Hz, 2H), 2.40 (t, $J = 5.6$ Hz, 2H), 1.76 (m, 2H), 1.69 (m, 2H).^{13}C NMR (150 MHz, $CDCl_3$) δ 153.7, 151.8, 140.8, 140.5, 137.4, 130.2, 128.9, 128.1, 127.5, 127.5, 127.1, 126.4, 116.3, 89.3, 44.2, 24.0, 24.0, 23.2, 22.2. HRMS (ESI+): *m/z* calcd for $C_{23}H_{21}N_3O^+$ $[M + H]^+$: 388.1484, found: 388.1453.

4.2.5.22. 1-Benzyl-3-(3-cyano-4,5,6,7-tetrahydrobenzo[b]thiophen-2-yl)-1-methylurea ***(9a)***. Yellow solid; yield 67.2%; m.p.: 115–116.5 ℃; Rf = 0.30 (EtOAc/petroleum ether = 1/5), ^{1}H NMR (600 MHz, $CDCl_3$) δ 7.53–7.48 (m, 1H), 7.36 (d, $J = 7.4$ Hz, 2H), 7.30 (t, $J = 8.3$ Hz, 3H), 4.59 (s, 2H), 3.07 (s, 3H), 2.59 (t, $J = 5.9$ Hz, 2H), 2.52 (t, $J = 5.9$ Hz, 2H), 1.82–1.76 (m, 4H). ^{13}C NMR (150 MHz, $CDCl_3$) δ 149.7, 136.4, 130.4, 129.1, 128.0, 127.5, 127.1, 114.9, 91.7, 52.7, 34.9, 23.9, 23.9, 23.2, 22.2. HRMS (ESI+): *m/z* calcd for $C_{18}H_{19}N_3O^+$ $[M + H]^+$: 326.1327, found: 326.1399.

4.2.5.23. 3-(3-Cyano-4,5,6,7-tetrahydrobenzo[b]thiophen-2-yl)-1-methyl-1-(2-methylbenzyl)urea ***(9b)***. Yellow solid; yield 51.1%; m.p.: 119.5–121.5 ℃; Rf = 0.55 (EtOAc/petroleum ether = 1/4), ^{1}H NMR (600 MHz, $CDCl_3$) δ 7.45 (s, 1H), 7.25–7.19 (m, 3H), 7.17 (dd, $J = 7.6$, 1.9 Hz, 1H), 4.61 (s, 2H), 3.04 (s, 3H), 2.59 (t, $J = 5.6$ Hz, 2H), 2.53 (t, $J = 5.6$ Hz, 2H), 2.32 (s, 3H), 1.83–1.76 (m, 4H).^{13}C NMR (150 MHz, $CDCl_3$) δ 153.4, 149.7, 136.4, 133.9, 131.1, 130.5, 128.1, 127.4, 127.2, 126.6, 114.9, 91.9, 50.6, 34.6, 24.1, 24.0, 23.3, 22.3, 19.3. HRMS (ESI+): *m/z* calcd for $C_{19}H_{21}N_3O^+$ $[M + H]^+$: 340.1484, found: 340.1489.

4.2.5.24. 3-(3-Cyano-4,5,6,7-tetrahydrobenzo[b]thiophen-2-yl)-1-methyl-1-(4-methylbenzyl)urea ***(9c)***. Yellow solid; yield 47.1%; m.p.: 103–104 ℃; Rf = 0.55 (EtOAc/petroleum ether = 1/4), ^{1}H NMR (600 MHz, $CDCl_3$) δ 7.46 (s, 1H), 7.22–7.15 (m, 4H), 4.54 (s, 2H), 3.07 (s, 3H), 2.59 (t, $J = 6.1$ Hz, 2H), 2.52 (t, $J = 6.1$ Hz, 2H), 2.34 (s, 3H), 1.85–1.75 (m, 4H).^{13}C NMR (150 MHz, $CDCl_3$) δ 153.4, 149.8, 137.9, 133.3, 130.5, 129.9, 127.6, 127.1, 115.0, 91.7, 52.6, 24.1, 24.0, 23.3, 22.3, 21.2. HRMS (ESI+): *m/z* calcd for $C_{19}H_{21}N_3O^+$ $[M + H]^+$: 340.1484, found: 340.1513.

4.2.5.25. 1-Benzyl-3-(3-cyano-4,5,6,7-tetrahydrobenzo[b]thiophen-2-yl)-1-ethylurea ***(9d)***. Yellow solid; yield 68.8%; m.p.: 109–110 ℃; Rf = 0.40 (EtOAc/petroleum ether = 1/6), ^{1}H NMR (600 MHz, $CDCl_3$) δ 7.42–7.36 (m, 3H), 7.33 (dd, $J = 7.8$, 2.7 Hz, 3H), 4.57 (s, 2H), 3.57–3.45 (m, 2H), 2.58 (t, $J = 6.2$ Hz, 2H), 2.51 (t, $J = 6.2$ Hz, 2H), 1.83–1.74 (m, 4H), 1.26 (t, $J = 7.2$ Hz, 3H).^{13}C NMR (150 MHz, $CDCl_3$) δ 153.1, 149.7, 136.5, 130.4, 129.3, 128.3, 127.4, 127.0, 114.8, 91.7, 50.7, 43.1, 24.0, 23.9, 23.3, 22.3, 13.5. HRMS (ESI+): *m/z* calcd for $C_{19}H_{21}N_3O^+$ $[M + H]^+$: 340.1484, found: 340.1517.

4.2.5.26. 1-Benzyl-3-(3-cyano-4,5,6,7-tetrahydrobenzo[b]thiophen-2-yl)-1-isopropylurea ***(9e)***. Yellow solid; yield 66.4%; m.p.: 118.5–120 ℃; Rf = 0.45 (EtOAc/petroleum ether = 1/6), ^{1}H NMR (600 MHz, $CDCl_3$) δ 7.42 (t, $J = 7.6$ Hz, 2H), 7.39–7.36 (m, 2H), 7.34 (t, $J = 7.3$ Hz, 1H), 7.28 (s, 1H), 4.78–4.70 (m, 1H), 4.46 (s, 2H), 2.55 (t, $J = 6.1$ Hz, 2H), 2.46 (t, $J = 6.1$ Hz, 2H), 1.80–1.72 (m, 4H), 1.28 (d, $J = 6.8$ Hz, 6H).^{13}C NMR (150 MHz, $CDCl_3$) δ 153.7, 149.5, 136.6, 130.5, 129.7, 128.5, 126.9, 126.8, 114.5, 91.6, 47.4, 45.8, 24.0, 23.9, 23.3, 22.3, 20.8. HRMS (ESI+): *m/z* calcd for $C_{20}H_{23}N_3O^+$ $[M + H]^+$: 354.1640, found: 354.1684.

4.2.5.27. 1,1-Dibenzyl-3-(3-cyano-4,5,6,7-tetrahydrobenzo[b]thiophen-2-yl)urea ***(9f)***. Yellow solid; yield 56.4%; m.p.: 167–168 ℃; Rf = 0.25 (EtOAc/petroleum ether = 1/6), ^{1}H NMR (600 MHz, $CDCl_3$) δ 7.45 (d, $J = 3.4$ Hz, 1H), 7.43–7.31 (m, 10*H*), 4.73–4.59 (m, 4H), 2.60 (d, $J = 6.0$ Hz, 2H), 2.50 (d, $J = 6.0$ Hz, 2H), 1.81–1.78 (m, 4H).^{13}C NMR (150 MHz, $CDCl_3$) δ 153.8, 149.4, 136.2, 130.6, 129.4, 128.4, 127.7, 127.1, 114.6, 92.0, 51.5, 24.0, 23.9, 23.3, 22.3. HRMS (ESI+): *m/z* calcd for $C_{24}H_{23}N_3O^+$ $[M + H]^+$: 388.1505, found: 388.1520.

4.2.5.28. 3-(3-Cyano-4,5,6,7-tetrahydrobenzo[b]thiophen-2-yl)-1-methyl-1-(naphthalen-1-ylmethyl)urea ***(9g)***. Yellow solid; yield 51.2%; m.p.: 151–152 ℃; Rf = 0.30 (EtOAc/petroleum ether = 1/6), ^{1}H NMR (600 MHz, $CDCl_3$) δ 8.04 (d, $J = 8.1$ Hz, 1H), 7.88 (dd, $J = 7.8$, 1.7 Hz, 1H), 7.84 (d, $J = 8.2$ Hz, 1H), 7.55–7.50 (m, 3H), 7.46 (dd, $J = 8.2$, 7.0 Hz, 1H), 7.39 (dd, $J = 7.0$, 1.2 Hz, 1H), 5.08 (s, 2H), 2.99 (s, 3H), 2.62 (t, $J = 5.6$ Hz, 2H), 2.53 (t, $J = 5.6$ Hz, 2H), 1.84–1.79 (m, 4H).^{13}C NMR (150

MHz, $CDCl_3$) δ 153.4, 149.7, 134.1, 131.7, 131.5, 130.6, 129.0, 129.0, 127.3, 126.9, 126.5, 126.3, 125.4, 123.4, 115.0, 92.1, 50.4, 33.8, 24.1, 24.0, 23.3, 22.3. HRMS (ESI+): *m/z* calcd for $C_{22}H_{21}N_3O^+$ $[M + H]^+$: 376.1484, found: 376.1527.

4.2.6. Synthesis of compounds ***2l-2q****, and* ***10a-10f***

Following the General method A, the intermediate **2l-2q** was prepared from compound **1h-1m** and malononitrile. Then, compounds **10a-10f** were obtained by treating the intermediate **2l-2q** with compound **6r** according to the General method B.

4.2.6.1. tert-butyl 2-amino-3-cyano-4,7-dihydrothieno[2,3-c]pyridine-6(5H)-carboxylate ***(2l)****.* Rf = 0.20 (EtOAc/petroleum ether = 1/4), ^{1}H NMR (600 MHz, $CDCl_3$) δ 4.35 (s, 2H), 3.64 (s, 2H), 2.57 (s, 2H), 1.46 (s, 9H). ESI-MS: *m/z* 280 $[M + H]^+$.

4.2.6.2. 2-Amino-6-hydroxy-4,5,6,7-tetrahydrobenzo[b]thiophene-3-carbonitrile ***(2m)****.* Rf = 0.75 (EtOAc/petroleum ether = 3/2), ^{1}H NMR (600 MHz, DMSO-d_6) δ 4.15 (t, *J* = 1.7 Hz, 2H), 3.36 (t, *J* = 6.1 Hz, 2H), 2.76 (td, *J* = 5.4, 4.8, 2.9 Hz, 2H). ESI-MS: *m/z* 195.1 $[M + H]^+$.

4.2.6.3. 2-Amino-9-methyl-5,6,7,8-tetrahydro-4H-5,8-epiminocyclohepta[b]thiophene-3-carbonitrile ***(2n)****.* Rf = 0.25 (MeOH/CH_2Cl_2 = 1/9), ^{1}H NMR (600 MHz, $CDCl_3$) δ 4.67 (d, *J* = 12.4 Hz, 2H), 3.74 (d, *J* = 5.2 Hz, 1H), 3.49 (s, 2H), 2.93 (dd, *J* = 16.6, 4.5 Hz, 1H), 2.39 (s, 3H), 1.94–1.88 (m, 1H), 1.59 (m, 1H), 0.86 (dt, *J* = 16.6, 7.9 Hz, 1H). ESI-MS: *m/z* 220 $[M + H]^+$.

4.2.6.4. 2-Amino-5,6,7,8-tetrahydro-4H-5,8-epiminocyclohepta[b]thiophene-3-carbonitrile ***(2o)****.* Rf = 0.25 (MeOH/CH_2Cl_2 = 1/9, +0.5% TEA), ^{1}H NMR (600 MHz, DMSO-d_6) δ 6.91 (s, 2H), 3.90 (d, *J* = 4.8 Hz, 1H), 3.69 (dd, *J* = 7.7, 4.4 Hz, 1H), 2.70 (dd, *J* = 16.1, 4.4 Hz, 1H), 2.09 (d, *J* = 16.1 Hz, 1H), 1.93 (m, 1H), 1.79 (m, 2H), 1.47–1.42 (m, 1H). ESI-MS: *m/z* 206 $[M + H]^+$.

4.2.6.5. 6-Acetyl-2-amino-4,5,6,7-tetrahydrothieno[2,3-c]pyridine-3-carbonitrile ***(2p)****.* Rf = 0.15 (MeOH/CH_2Cl_2 = 5/95), ^{1}H NMR (600 MHz, DMSO-d_6) δ 7.30 (d, *J* = 10.9 Hz, 2H), 4.48 (d, *J* = 22.6 Hz, 2H), 3.78 (dt, *J* = 18.4, 5.8 Hz, 2H), 2.63 (tt, *J* = 3.5, 2.2 Hz, 2H), 2.17 (d, *J* = 28.8 Hz, 3H). ESI-MS: *m/z* 222 $[M + H]^+$.

4.2.6.6. 2-amino-5,5,7,7-tetramethyl-4,5,6,7-tetrahydrothieno[2,3-c]pyridine-3-carbonitrile ***(2q)****.* Rf = 0.35 (MeOH/CH_2Cl_2 = 1/9), ^{1}H NMR (600 MHz, DMSO-d_6) δ 7.03 (s, 2H), 2.18 (s, 2H), 1.24 (s, 6H), 1.08 (s, 6H). ESI-MS: *m/z* 236 $[M + H]^+$.

4.2.6.7. Tert-butyl 3-cyano-2-(3-(2,4-dimethoxybenzyl)ureido)-4,7-dihydrothieno[2,3-c]pyridine-6(5H)-carboxylate ***(10a)****.* White solid; yield 49.9%; m.p.: 173–174.5 ℃; Rf = 0.15 (EtOAc/petroleum ether = 1/2), ^{1}H NMR (600 MHz, $CDCl_3$) δ 8.74 (s, 1H), 7.17 (d, *J* = 8.2 Hz, 1H), 6.43–6.36 (m, 2H), 6.18 (s, 1H), 4.43–4.35 (m, 4H), 3.77 (d, *J* = 7.6 Hz, 6H), 3.65 (s, 2H), 2.53 (s, 2H), 1.47 (s, 9H). $_{13}$C NMR (150 MHz, DMSO-d_6) δ 160.1, 158.0, 153.9, 153.2, 151.4, 129.4, 128.8, 118.7, 114.5, 104.3, 98.4, 88.0, 79.4, 55.5, 55.2, 38.4, 28.0. HRMS (ESI+): *m/z* calcd for $C_{23}H_{28}N_4O_5^+$ $[M + H]^+$: 473.1859, found: 473.1859.

4.2.6.8. 1-(3-Cyano-6-hydroxy-4,5,6,7-tetrahydrobenzo[b]thiophen-2-yl)-3-(2,4-dimethoxybenzyl)urea ***(10b)****.* White solid; yield 62.7%; m.p.: 231–233 ℃; Rf = 0.25 (EtOAc/petroleum ether = 3/2), ^{1}H NMR (600 MHz, DMSO-d_6) δ 9.94 (s, 1H), 7.12 (d, *J* = 8.3 Hz, 1H), 7.03 (t, *J* = 5.8 Hz, 1H), 6.57 (d, *J* = 2.4 Hz, 1H), 6.48 (dd, *J* = 8.3, 2.4 Hz, 1H), 4.91 (d, *J* = 4.1 Hz, 1H), 4.18 (d, *J* = 5.7 Hz, 2H), 3.96–3.89 (m, 1H), 3.82 (s, 3H), 3.74 (s, 3H), 2.76 (dd, *J* = 15.9, 4.9 Hz, 1H), 2.58–2.52 (m, 1H), 2.44 (ddd, *J* = 15.9, 7.8, 5.8 Hz, 1H), 2.41–2.35 (m, 1H), 1.88–1.81 (m, 1H), 1.69–1.62 (m, 1H).^{13}C NMR (150 MHz, DMSO-d_6) δ 160.1, 158.0, 153.3, 150.9, 129.4, 129.2, 122.7, 118.8, 114.9, 104.3, 98.4, 88.1, 65.2, 55.5, 55.2, 38.4, 32.4, 30.1, 21.4. HRMS (ESI+): *m/z* calcd for $C_{19}H_{21}N_3O_4^+$ $[M + H]^+$: 388.1331, found: 388.1334.

4.2.6.9. 1-(3-Cyano-9-methyl-5,6,7,8-tetrahydro-4H-5,8-epiminocyclohepta[b]thiophen-2-yl)-3-(2,4-dimethoxybenzyl)urea ***(10c)****.* Brown solid; yield 51.5%; m.p.: 176–178 ℃; Rf = 0.70 (MeOH/CH_2Cl_2 = 15/85), ^{1}H NMR (600 MHz, $CDCl_3$) δ 8.63 (s, 1H), 7.18 (d, *J* = 8.2 Hz, 1H), 6.43 (d, *J* = 2.4 Hz, 1H), 6.40 (dd, *J* = 8.2, 2.4 Hz, 1H), 6.08 (t, *J* = 5.9 Hz, 1H), 4.37 (d, *J* = 5.9 Hz, 2H), 3.81 (s, 3H), 3.78 (s, 3H), 3.77 (s, 1H), 3.45 (dd, *J* = 7.4, 4.4 Hz, 1H), 2.87 (dd, *J* = 16.6, 4.4 Hz, 1H), 2.32 (s, 3H), 2.26–2.14 (m, 2H), 2.09 (d, *J* = 16.6 Hz, 1H), 1.89–1.83 (m, 1H), 1.51 (ddd, *J* = 11.4, 8.8, 5.4 Hz, 1H). ^{13}C NMR (150 MHz, $CDCl_3$) δ 160.6, 158.5, 153.6, 151.7, 130.3, 128.6, 125.5, 119.0, 115.7, 103.8, 98.6, 58.9, 56.7, 55.5, 55.5, 39.9, 35.9, 35.2, 29.6, 28.8. HRMS (ESI+): *m/z* calcd for $C_{21}H_{24}N_4O_3^+$ $[M + H]^+$: 413.1647, found: 413.1648.

4.2.6.10. 1-(3-Cyano-5,6,7,8-tetrahydro-4H-5,8-epiminocyclohepta[b]thiophen-2-yl)-3-(2,4-dimethoxybenzyl)urea ***(10d)****.* Brown solid; yield 43.2%; m.p.: 123–124 ℃; Rf = 0.20 (MeOH/CH_2Cl_2 = 1/9), ^{1}H NMR (600 MHz, DMSO-d_6) δ 7.11 (d, *J* = 8.3 Hz, 1H), 7.06 (t, *J* = 5.8 Hz, 1H), 6.57 (d, *J* = 2.4 Hz, 1H), 6.48 (dd, *J* = 8.3, 2.4 Hz, 1H), 4.25 (d, *J* = 5.3 Hz, 1H), 4.19 (d, *J* = 5.8 Hz, 2H), 3.86 (dd, *J* = 7.8, 4.6 Hz, 1H), 3.81 (s, 3H), 3.74 (s, 3H), 2.84 (dd, *J* = 16.3, 4.6 Hz, 1H), 2.30 (dd, *J* = 16.3, 1.2 Hz, 1H), 1.99 (s, 1H), 1.91 (dp, *J* = 11.2, 5.9 Hz, 1H), 1.83 (ddd, *J* = 11.6, 8.9, 2.5 Hz, 1H), 1.54–1.48 (m, 1H). ^{13}C NMR (150 MHz, DMSO-d_6) δ 160.1, 158.0, 153.3, 150.4, 129.8, 129.4, 126.2, 118.8, 114.7, 104.3, 98.4, 88.6, 55.5, 55.3, 52.7, 51.9, 38.4, 36.3, 33.3, 28.5. HRMS (ESI+): *m/z* calcd for $C_{20}H_{22}N_4O_3^+$ $[M + H]^+$: 399.1491, found: 399.1486.

4.2.6.11. 1-(6-Acetyl-3-cyano-4,5,6,7-tetrahydrothieno[2,3-c]pyridin-2-yl)-3-(2,4-dimethoxybenzyl)urea ***(10e)****.* White solid; yield 62.3%; m.p.: 205–206 ℃; Rf = 0.50 (MeOH/CH_2Cl_2 = 5/95), ^{1}H NMR (600 MHz, DMSO-d_6) δ 10.08 (s, 1H), 7.12 (d, *J* = 8.3 Hz, 1H), 7.06 (t, *J* = 5.6 Hz, 1H), 6.57 (d, *J* = 2.2 Hz, 1H), 6.48 (dt, *J* = 8.3, 1.8 Hz, 1H), 4.49 (dt, *J* = 27.7, 1.8 Hz, 2H), 4.19 (dd, *J* = 5.8, 3.6 Hz, 2H), 3.82 (s, 3H), 3.74 (s, 3H), 3.68 (dt, *J* = 18.0, 5.8 Hz, 2H), 2.61 (td, *J* = 5.5, 2.8 Hz, 1H), 2.49–2.46 (m, 1H), 2.06 (d, *J* = 24.8 Hz, 3H). ^{13}C NMR (150 MHz, DMSO-d_6) δ 168.9, 168.7, 160.1, 158.0, 153.2, 153.2, 151.4, 129.5, 129.4, 128.8, 121.7, 121.4, 118.7, 114.6, 104.4, 98.4, 87.9, 55.6, 55.3, 43.9, 42.8, 38.5, 37.9, 24.3, 23.4, 21.8, 21.3. HRMS (ESI+): *m/z* calcd for $C_{20}H_{22}N_4O_4^+$ $[M + H]^+$: 415.1440, found: 415.1450.

4.2.6.12. 1-(3-Cyano-5,5,7,7-tetramethyl-4,5,6,7-tetrahydrothieno[2,3-c]pyridin-2-yl)-3-(2,4-dimethoxybenzyl)urea ***(10f)****.* Brown solid; yield 60.1%; m.p.: 92–93 ℃; Rf = 0.15 (MeOH/CH_2Cl_2 = 5/95), ^{1}H NMR (600 MHz, DMSO-d_6) δ 10.03 (s, 1H), 7.11 (d, *J* = 8.3 Hz, 1H), 7.07 (t, *J* = 5.9 Hz, 1H), 6.57 (d, *J* = 2.4 Hz, 1H), 6.48 (dd, *J* = 8.3, 2.4 Hz, 1H), 4.18 (d, *J* = 5.8 Hz, 2H), 3.82 (s, 3H), 3.74 (s, 3H), 2.28 (s, 2H), 1.31 (s, 6H), 1.09 (s, 6H). ^{13}C NMR (150 MHz, DMSO-d_6) δ 160.1, 158.0, 153.3, 150.8, 132.5, 129.4, 127.6, 118.9, 115.1, 104.3, 98.4, 88.4, 55.6, 55.3, 51.7, 49.8, 38.4, 36.7, 33.6, 29.6. HRMS (ESI+): *m/z* calcd for $C_{22}H_{28}N_4O_3^+$ $[M + H]^+$: 429.1960, found: 429.1966.

4.3. α-Glucosidase inhibition bioassay

The inhibitory activity against α-glucosidase of tested compounds was performed according to the reported methods [10,36]. Acarbose was used as a positive control. The tested compounds and acarbose were respectively dissolved in DMSO, while the enzyme and the substrate were both dissolved in PBS (pH = 6.8). After pre-incubation of tested compounds with α-glucosidase in PSB (37 °C, 15 min), 25 μL substrate buffers were added to the system and the incubation was continued at 37 °C for another 15 min. Finally, the reaction was terminated by the

addition of 50 μL 0.2 M sodium carbonate solution. The optical density (OD) was measured at an absorbance wavelength of 405 nm using a Microplate Reader (Tecan, Switzerland). The calculation formula of the inhibition rate is: % inhibition rate = $[(A_1 - A_0)/A_0] \times 100\%$, where A_1 and A_0 are the absorbance of the test compound with or without. The IC_{50} value is determined from the graph of the relationship between the inhibition rate and the different concentration of the test compound. The experiment was performed in triplicate.

4.4. α-Amylase inhibition bioassay

The α-amylase activity of compounds was assessed based on a previously reported protocolwith slight modification [42]. The tested compounds and acarbose were respectively dissolved in DMSO, and porcine pancreatic α-amylase (EC 3.2.1.1) was dissolved in 0.1 M phosphate buffer at pH 6.8. After 10 min of incubation of 75 μL of the enzyme solution and 75 μL of tested compound solution at 25 °C, 75 μL of the starch solution (0.1% p/v in 0.1 M phosphate buffer at pH 6.8) was added to start the reaction and the mixture were incubated for 10 min at 25 °C. Then the reaction was stopped by the addition of 62.5 μL dinitrosalicylic (DNS) reagent. The optical density (OD) was measured at an absorbance wavelength of 580 nm using a Tecan Microplate Reader. The absorbance was recorded at 580 nm using a microplate reader. The calculation formula of the inhibition rate is: % inhibition rate = $[(A_0 - A_1)/A_0] \times 100\%$, where A_0 was the absorbance without tested compound, A_1 was the absorbance of the tested compound at different concentrations.

4.5. Fluorescence quenching experiment

The fluorescence quenching experiment was referred to a reported protocol [43]. Briefly, α-glucosidase (1U/mL) was pre-treated with certain concentrations of inhibitors for 30 min at 37 °C in the fluorescence spectrophotometer (Agilent Cary Eclipse). Then 100 μL of the above solution (pH 6.8) was added accurately to the quartz cell. The blank was used for buffer spectrum values. The excitation wavelength was 290 nm, and the emission spectrum was recorded from 300 to 420 nm at 37 °C.

4.6. Kinetics of α-glucosidase inhibitors

Inhibition type of inhibitors towards α-glucosidase was studied according to a described method [44]. Increasing concentrations of pNPG were used as substrates in the absence or presence of tested compounds at four different concentrations around the IC50 values. The inhibitory kinetics of the investigated compounds on α-glucosidase was analyzed using the Lineweaver-Burk plot of the substrate concentration and velocity.

4.7. Molecular modeling

The online program SWISS MODEL (https://swissmodel.expasy.org/) was used to perform homology modelling. First, the primary amino acid sequence of α-glucosidase (*Saccharomyces cerevisiae* organism, EC:3.2.1.20) was uploaded to the program, then the SWISS-MODEL template library (STML, last update: 2021-03-31, last included PDB release: 2021-03-26) was searched with BLAST [45] and HHBlits [46] for evolutionary related structures matching the uploaded sequence (target sequence) when the Search For Templates was performed. Next, according to the reported result, the template was chosen for homology modelling of α-glucosidase crystal structure. Model was built based on the target-template alignment using ProMod3. Coordinates which are conserved between the target and the template are copied from the template to the model. Insertions and deletions are remodeled using a fragment library. Side chains are then rebuilt. Finally, the geometry of the resulting model is regularized by using a force field. The global and per-residue model quality has been assessed using the QMEAN scoring function [47]. The built model was selected for the following molecular docking simulation.

Molecular docking simulation was performed with Glide (grid-based ligand docking with energetics) program. Firstly, the ligands were prepared by the LigPrep module (LigPrep, version 3.4) in Schrodinger software (Schrodinger, LLC: New York, NY, 2015). Next, the coordinates of modeled α-glucosidase protein structure were optimized by the module of Protein Preparation Wizard module in the Maestro program (Maestro, version 10). Then the protein grid files were generated with the Receptor Grid Generation module. Finally, the prepared ligands were docked to the protein grid files with the XP precision mode. The top-ranking pose was selected for binding mode analysis.

4.8. Molecular dynamics (MD) simulation

MD simulation was performed to verify stability of constructed homology model. H^{++} program [48] was used to predict the protonation states of all ionizable residues. A periodic box of transferable intermolecular potential 3P water molecules that extended 10.0 Å from the protein atoms was used. Counter-ions (Na^+) were added to neutralize the simulation system. AMBER 14.0 package [49] was used to perform MD simulations. Isothermal-isobaric (NPT) ensemble and periodic boundary conditions were used. The force field for this simulation was Amber14SB. SHAKE algorithm [50] and particle-mesh Ewald method [51] were respectively used to constrain small bonds involving hydrogen atoms and to calculate the electrostatic interactions. The non-bonded pairs were updated every 25 steps while the non-bonded cutoff was set to 10 Å. 2 ns MD simulation was coupled to a 300 K thermal bath at 1 bar pressure by using the algorithm of Berendsen et al. [52].

4.9. Prediction of druglikeness properties

The pharmacokinetic properties of 8r and 8s were predicted by the "ADMET Descriptors" module implemented in DS3.0 [53] and online molinspiration [54].

4.10. Cell viability assay

The HepG2 and LO2 cell lines were cultured in a proper medium supplemented with 10% fetal bovine serum in a humidified atmosphere of 5% CO_2 at 37 °C. Cell suspensions were plated in 96-well plates at a density of 2×10^4 cells/cm^3. After incubation for 24 h, the cells were treated with various concentrations of tested substances for 48 h and then incubated with 100 μL of MTT at 37 °C for 2 h. The formazan dye product was measured by the absorbance at 490 nm on a Tecan Spark multimode microplate reader (Switzerland).

4.11. Hypoglycemic activity assay

Experiments were performed in 190 ~ 220 g SD rats (Jinan Pengyue Experimental Animal Breeding Co. Ltd, Jinan, Shandong, China) housed in groups of 6 on a 12 h/12 h light–dark schedule cycle. All *in vivo* experiments followed the ARRIVE guidelines [55]. After 3 days of stabilization, in each experimental group, 12 SD rats were used. Each tested group received a dose of acarbose and tested compound (5 mg/kg), and then 7.5 g/kg sucrose solution was given 30 min after oral administration; the control group was only received the sucrose solution. Blood samples were collected from the tail vein before and after sucrose administration at 10, 20, 30, 45, 60, 90, and 120 min. The plasma glucose was recorded using glucometer (Roche, Accu-chek performa).

4.12. Data analysis

Data are presented as mean ± SD, and at least three independent replications were performed. Images were processed by use of GraphPad

Prism 5 (GraphPad Software, La Jolla, CA, USA). One-way ANOVA combined with Bonferroni post hoc tests were used to determine the significance between different groups. $P < 0.05$ was considered statistically significant. For *in vivo* experiments, the level of blood glucose was expressed in mmol/L, and the areas under the curve (AUC) for 120 min were established.

Declaration of Competing Interest

The authors declare that they have no known competing financial interests or personal relationships that could have appeared to influence the work reported in this paper.

Acknowledgements

This research work was financially supported by Natural Science Foundation of Shandong Province [Nos. ZR2019YQ31; ZR2020MB103], National Natural Science Foundation of China [No. 21672082], Major Science and Technology Innovation Project of Shandong Province [No. 2019JZZY011116], and the Science and Technology Project of University of Jinan [No. XKY2004].

Appendix A. Supplementary material

Supplementary data to this article can be found online at https://doi.org/10.1016/j.bioorg.2021.105236.

References

[1] Z.A. Ma, Z. Zhao, J. Turk, Mitochondrial dysfunction and β-cell failure in type 2 diabetes mellitus, Exp. Diabetes Res. 2012 (2012), 703538.
[2] M. Dhameja, P. Gupta, Synthetic heterocyclic candidates as promising α-glucosidase inhibitors: An overview, Eur. J. Med. Chem. 176 (2019) 343–377.
[3] IDF Diabetes Atlas 9th Edition. https://www.idf.org/aboutdiabetes/what-is-diabetes/facts-figures.html. 2019.
[4] D. Milonas, T. Didangelos, A.I. Hatzitolios, K. Tziomalos, Incretin-based antihyperglycemic agents for the management of acute ischemic stroke in patients with diabetes mellitus: a review, Diabetes Ther. 10 (2019) 429–435.
[5] J.C. Khoury, D. Kleindorfer, K. Alwell, C.J. Moomaw, D. Woo, O. Adeoye, M. L. Flaherty, P. Khatri, S. Ferioli, J.P. Broderick, B.M. Kissela, Diabetes mellitus: a risk factor for ischemic stroke in a large biracial population, Stroke 44 (2013) 1500–1504.
[6] S.P. Marso, W.R. Hiatt, Peripheral arterial disease in patients with diabetes, J. Am. Coll. Cardiol. 47 (2006) 921–929.
[7] E.J. Gallagher, D. LeRoit, Obesity and diabetes: the increased risk of cancer and cancer-related mortality, Physiol. Rev. 95 (2015) 727–748.
[8] J.B. Cole, J.C. Florez, Genetics of diabetes mellitus and diabetes complications, Nat. Rev. Nephrol. 16 (2020) 377–390.
[9] A.K. Mandal, Diabetes, In treating diabetes, what is important? Glucose levels or outcome measures? World J. Diabetes. 6 (2015) 1243–1245.
[10] G.J. Ye, T. Lan, Z.X. Huang, X.N. Cheng, C.Y. Cai, S.M. Ding, M.L. Xie, B. Wang, Design and synthesis of novel xanthone-triazole derivatives as potential antidiabetic agents: α-Glucosidase inhibition and glucose uptake promotion, Eur. J. Med. Chem. 177 (2019) 362–373.
[11] A.J. Hirsh, S.Y. Yao, J.D. Young, C.I. Cheeseman, Inhibition of glucose absorption in the rat jejunum: A novel action of alpha-D-glucosidase inhibitors, Gastroenterology 113 (1997) 205–211.
[12] J.H. Kim, H.Y. Kim, C.H. Jin, Mechanistic investigation of anthocyanidin derivatives as α-glucosidase inhibitors, Bioorg. Chem. 87 (2019) 803–809.
[13] S.A. Ross, E.A. Gulve, M. Wang, Chemistry and biochemistry of type 2 diabetes, Chem. Rev. 104 (2004) 1255–1282.
[14] H. Bischoff, Pharmacology of alpha-glucosidase inhibition, Eur. J. Clin. Invest. 3 (1994) 3–10.
[15] Y.S. Lee, M.H. Lee, H.S. Lee, S.J. Lee, Y.W. Kim, R. Zhang, S.G. Withers, K.S. Kim, S. J. Lee, K.H. Park, Enzymatic synthesis of a selective inhibitor for alpha-glucosidases: alpha-acarviosinyl-(1–>9)-3-alpha-D-glucopyranosylpropen, J. Agric. Food Chem. 56 (2008) 5324–5330.
[16] H. Bischoff, The mechanism of alpha-glucosidase inhibition in the management of diabetes, Clin. Invest. Med. 18 (1995) 303–311.
[17] S.R. Joshi, E. Standl, N. Tong, P. Shah, S. Kalra, R. Rathod, Therapeutic potential of α-glucosidase inhibitors in type 2 diabetes mellitus: an evidence-based review, Expert Opin. Pharmacother. 16 (2015) 1959–1981.
[18] D. Sacks, B. Baxter, B.C.V. Campbell, J.S. Carpenter, C. Cognard, D. Dippel, M. Eesa, U. Fischer, K. Hausegger, J.A. Hirsch, M.S. Hussain, O. Jansen, M. V. Jayaraman, A.A. Khalessi, B.W. Kluck, S. Lavine, P.M. Meyers, S. Ramee, D. A. Rüfenacht, C.M. Schirmer, D. Vorwerk, Multisociety consensus quality improvement revised consensus statement for endovascular therapy of acute ischemic stroke, Int. J. Stroke. 13 (2018) 612–632.
[19] B. Usman, N. Sharma, S. Satija, M. Mehta, M. Vyas, G.L. Khatik, N. Khurana, P. M. Hansbro, K. Williams, K. Dua, Recent developments in alpha-glucosidase inhibitors for management of type-2 diabetes: an update, Curr. Pharm. Des. 25 (2019) 2510–2525.
[20] U. Hossain, A.K. Das, S. Ghosh, P.C. Sil, An overview on the role of bioactive α-glucosidase inhibitors in ameliorating diabetic complications, Food Chem. Toxicol. 145 (2020), 111738.
[21] J.M. Wang, S.l. Lu, R.L. Sheng, J.T. Fan, W.H. Wu, R.H. Guo, Structure-activity relationships of natural and synthetic indole-derived scaffolds as α-glucosidase inhibitors: A mini-review, Mini. Rev. Med. Chem. 20 (2020) 1791-1818.
[22] M.T. Javid, F. Rahim, M. Taha, H. Ur Rehman, M. Nawaz, A. Wadood, S. Imran, I. Uddin, A. Mosaddik, K.M. Khan, Synthesis, in vitro α-glucosidase inhibitory potential and molecular docking study of thiadiazole analogs, Bioorg. Chem. 78 (2018) 201–209.
[23] M. Taha, S.A.A. Shah, M. Afifi, S. Imran, S. Sultan, F. Rahim, K.M. Khan, Synthesis, α-glucosidase inhibition and molecular docking study of coumarin based derivatives, Bioorg. Chem. 77 (2018) 586–592.
[24] M. Taha, S. Imran, F. Rahim, A. Wadood, K.M. Khan, Oxindole based oxadiazole hybrid analogs: Novel α-glucosidase inhibitors, Bioorg. Chem. 76 (2018) 273–280.
[25] M. Taha, S. Imran, M. Salahuddin, N. Iqbal, F. Rahim, N. Uddin, A. Shehzad, R. K. Farooq, M. Alomari, K.M. Khan, Evaluation and docking of indole sulfonamide as a potent inhibitor of α-glucosidase enzyme in streptozotocin -induced diabetic albino wistar rats, Bioorg. Chem. 110 (2021), 104808.
[26] I. Khan, A. Khan, S.A. Halim, M. Khan, S. Zaib, B.E.M. Al-Yahyaei, A. Al-Harrasi, A. Ibrar, Utilization of the common functional groups in bioactive molecules: Exploring dual inhibitory potential and computational analysis of keto esters against α-glucosidase and carbonic anhydrase-II enzymes, Int. J. Biol. Macromol. 167 (2021) 233–244.
[27] M. Kazmi, S. Zaib, S.T. Amjad, I. Khan, A. Ibrar, A. Saeed, J. Iqbal, Exploration of aroyl/heteroaroyl iminothiazolines featuring 2,4,5-trichlorophenyl moiety as a new class of potent, selective, and in vitro efficacious glucosidase inhibitors, Bioorg. Chem. 74 (2017) 134–144.
[28] Y.Y. Zhong, H.S. Chen, P.P. Wu, B.J. Zhang, Y. Yang, Q.Y. Zhu, C.G. Zhang, S. Q. Zhao, Synthesis and biological evaluation of novel oleanolic acid analogues as potential α-glucosidase inhibitors, Eur. J. Med. Chem. 164 (2019) 706–716.
[29] S. Ganesan, Isolation and screening of a-glucosidase enzyme inhibitor producing marine actinobacteria, Afr. J. Microbiol. Res. 5 (2011) 21–30.
[30] U. Ghani, M. Nur-E-Alam, M. Yousaf, Z. Ul-Haq, O.M. Noman, A.J. Al-Rehaily, Natural flavonoid α-glucosidase inhibitors from Retama raetam: Enzyme inhibition and molecular docking reveal important interactions with the enzyme active site, Bioorg. Chem. 87 (2019) 736–742.
[31] U. Ghani, Alpha-Glucosidase Inhibitors, Clinically Promising candidateds for Anti-Diabetic Drug Discovery, Elsevier. 2020, pp. 1-5.
[32] H. Seino, H. Yamaguchi, A. Misaki, Y. Sakata, M. Kitagawa, T. Yamazaki, H. Kikuchi, R. Abe, Opinion, Clinical effect of combination therapy of pioglitazone and an α-glucosidase inhibitor, Curr. Med. Res. Opin. 19 (2003) 675–682.
[33] G. Derosa, P. Maffioli, α-Glucosidase inhibitors and their use in clinical practice, Arch. Med. Sci. 8 (2012) 899–906.
[34] T.T. Chai, M.T. Kwek, H.C. Ong, F.C. Wong, Water fraction of edible medicinal fern Stenochlaena palustris is a potent α-glucosidase inhibitor with concurrent antioxidant activity, Food Chem. 186 (2015) 26–31.
[35] M.J. Wu, H. Wang, C.S. Jiang, Y.W. Guo, New cembrane-type diterpenoids from the South China Sea soft coral Sinularia crassa and their α-glucosidase inhibitory activity, Bioorg. Chem. 104 (2020), 104281.
[36] S.K. Liu, H.F. Hao, Y. Bian, Y.X. Ge, S.Y. Lu, H.X. Hie, J. Zhang, J. Zhang, C. S. Jiang, K.K. Zhu, Discovery of new α-glucosidase inhibitors: structure-based virtual screening and biological evaluation, Front. Chem. 9 (2021), 639279.
[37] M.S.H. Salem, Y.M.A. Aziz, M.S. Elgawish, M.M. Said, K.A.M. Abouzid, Design, synthesis, biological evaluation and molecular modeling study of new thieno[2,3-d]pyrimidines with anti-proliferative activity on pancreatic cancer cell lines, Bioorg. Chem. 94 (2020), 103472.
[38] J. Venter, C. Perez, W.A.L. Otterlo, A. Martínez, M.A.L. Blackie, 1-Aryl-3-(4-methoxybenzyl)ureas as potentially irreversible glycogen synthase kinase 3 inhibitors: Synthesis and biological evaluation, Bioorg. Med. Chem. Lett. 29 (2019) 1597–1600.
[39] D. Shahzad, A. Saeed, F.A. Larik, P.A. Channar, Q. Abbas, M.F. Alajmi, M.I. Arshad, M.F. Erben, M. Hassan, H. Raza, S.Y. Seo, H.R. El-Seedi, Novel C-2 symmetric molecules as α-glucosidase and α-amylase inhibitors: design, synthesis, kinetic evaluation, molecular docking and pharmacokinetics, Molecules 24 (2019) 1511.
[40] P. Lin, J.C. Zeng, J.G. Chen, X.L. Nie, E. Yuan, X.Q. Wang, D.Y. Peng, Z.P. Yin, Synthesis, in vitro inhibitory activity, kinetic study and molecular docking of novel N-alkyl-deoxynojirimycin derivatives as potential α-glucosidase inhibitors, J. Enzyme Inhib. Med. Chem. 35 (2020) 1879–1890.
[41] T. Mosmann, Rapid colorimetic assay for cellular growth and survival: Application to proliferation and cytotoxicity assays, J. Immunol. Methods 65 (1983) 55–63.
[42] S. Adisakwattana, T. Ruengsamran, P. Kampa, W. Sompong, In vitro inhibitory effects of plant-based foods and their combinations on intestinal α-glucosidase and pancreatic α-amylase, BMC. Complement Altern. Med. 31 (2012) 110.
[43] M. Aguilar-Moncayo, M.I. García-Moreno, A.E. Stütz, J.M.G. Fernández, T. M. Wrodnigg, C.O. Mellet, Fluorescent-tagged sp2-iminosugars with potent β-glucosidase inhibitory activity, Bioorg. Med. Chem. 18 (2010) 7439–7445.
[44] W.L. Hou, Y.F. Li, Q. Zhang, X. Wei, A.H. Peng, L.J. Chen, Y.Q. Wei, Triterpene acids isolated from Lagerstroemia speciosa leaves as alpha-glucosidase inhibitors, Phytother. Res. 23 (2009) 614–618.

[45] C. Camacho, G. Coulouris, V. Avagyan, M. Ning, T.L.J.B.B. Madden, BLAST+: architecture and applications, BMC Bioinformatics. 10 (2009) 421-429.
[46] M. Remmert, A. Biegert, A. Hauser, J.J.N.M. Sding, HHblits: lightning-fast iterative protein sequence searching by HMM-HMM alignment, Nat. Methods. 9 (2011) 173–175.
[47] S. Gabriel, R. Christine, A.M. Waterhouse, G. Rafal, H. Juergen, S. Torsten, QMEANDisCo - distance constraints applied on model quality estimation, Bioinformatics 36 (2020) 1765–1771.
[48] J.C. Gordon, J.B. Myers, T. Folta, V. Shoja, L.S. Heath, A. Onufriev, H++: a server for estimating pKas and adding missing hydrogens to macromolecules, Nucleic Acids Res. 33 (2005) W368–W371.
[49] D.A. Case, T.E. Cheatham 3rd, T. Darden, H. Gohlke, R. Luo, K.M. Merz Jr., A. Onufriev, C. Simmerling, B. Wang, R.J. Woods, The Amber biomolecular simulation programs, J. Comput. Chem. 26 (2005) 1668–1688.
[50] J.P. Ryckaert, G. Ciccotti, H.J.C. Berendsen, Numerical integration of the Cartesian equations of motion of a system with constraints: molecular dynamics of n-alkanes, J. Comput. Phys. 23 (1977) 327–341.
[51] T. Darden, Y. Darrin, L. Pedersen, Particle mesh Ewald: An N·log(N) method for Ewald sums in large systems, J. Chem. Phys. 98 (1993) 10089–10092.
[52] H.J.C. Berendsen, J.P.M. Postma, W.F.V. Gunsteren, A. Dinola, J.R. Haak, Molecular dynamics with coupling to an external bath, J. Chem. Phys. 81 (1984) 3684–3690.
[53] Accelrys Discovery Studio 3.0, Accelrys, San Diego, CA, 2010.
[54] https://molinspiration.com/cgi-bin/properties#.
[55] C. Kilkenny, W.J. Biology, I. Cuthi, M. Emerson, D.G. Altman, Improving bioscience research reporting: the ARRIVE guidelines for reporting animal research, Vet. Clin. Pathol. 41 (2012) 27–31.